DETERMINATION OF LIVE AND DEAD BACTERIA WITH A NOVEL HANDHELD

INSTRUMENT AND RAMAN SPECTROSCOPY

A Thesis

by

DINESH DHANKHAR

Submitted to the Office of Graduate and Professional Studies of
Texas A&M University
in partial fulfillment of the requirements for the degree of

MASTER OF SCIENCE

Chair of Committee,	Peter Rentzepis
Committee Members,	Laszlo Kish
	Maria King
	Edward Dougherty
	Krishna Narayanan
Head of Department,	Miroslav Begovic

December 2018

Major Subject: Electrical Engineering

ABSTRACT

Fast identification of live and dead (inactivated) bacteria in situ, whether it is a hospital or field, is a challenging problem. Typically, counting live and dead bacteria requires more than 24 hours (for plating, CFU growth and counting etc.), during which time bacterial infections can grow many fold (bacteria can double in as short as 10 minutes times). In this research, a handheld instrument was designed and constructed which can be carried to the field and can be used for in-situ detection of live and dead bacteria ratio within a few minutes. This handheld instrument is based on the detection of fluorescence from tryptophan and tyrosine present in bacteria. As bacteria are inactivated by UV radiation, fluorescence from tryptophan and tyrosine decreases. By measuring this fluorescence using the developed handheld device, it was possible to determine live and dead bacteria in a sample.

Alongside, Raman spectroscopy was explored to determine live and dead bacteria after ultraviolet light inactivation. It was found that there exist a quantitative relationship between changes in Raman spectra of bacteria and number of inactivated cells in a sample.

DEDICATION

To Dr. Rajbir Singh Dhankhar

(1956 - 2016)

ACKNOWLEDGEMENTS

TABLE OF CONTENTS

LIST OF FIGURES

LIST OF TABLES

CHAPTER I

INTRODUCTION TO THESIS

It has been shown earlier [1] that UV (ultraviolet) fluorescence of bacteria (primarily coming from tryptophan and tyrosine in proteins) can be used to determine live and dead bacteria ratio. This technique was studied in more detail to understand the mechanism behind the bacterial inactivation and to make a new, novel handheld instrument.

This hand-held instrument is capable of measuring bacterial UV fluorescence and classifying live and dead bacteria using PCA (Principal Component Analysis). This device was designed and constructed in order to be used in the field for fast (minutes), in-situ measurements. This instrument uses a UV LED to excite the bacteria fluorescence as well as inactivation of the bacteria.

Along with this, Raman spectroscopy of *E.coli* bacteria before and after UV irradiation was performed in order to study the feasibility of Raman spectroscopy to determine live and dead bacteria. This was done because Raman spectra can give more information at a molecular level compared to fluorescence spectra. It was found using Raman spectroscopy that proteins, along with DNA bases are the major components undergoing changes after UV irradiation. UV induced photoproducts were detected in Raman spectra and a quantitative relationship between increase in photoproducts and fraction of dead (inactivated) bacteria was established. Raman spectroscopy was also used to identify different bacterial strains. Currently, Raman spectroscopy capability is also being added into the handheld device.

This thesis is organized into six chapters. Chapter II provides background to various spectroscopic and statistical techniques used in this research along with a background about

bacteria. Chapter III is concerned with the design and construction of the handheld instrument. Chapter IV describes methods and materials used for Raman spectroscopy experiments and for testing the handheld instrument. Chapter V describes results and discussions and Chapter VI provides conclusion.

CHAPTER II

BACKGROUND

Healthcare Associated Infection (HAI) is among the top 10 causes of death in the United States [5]. It has been estimated that 5 to 10 % of hospitalized patients develop HAI. The majority of HAI is due to bacteria and for preventing these infections, rapid identification of live and dead (inactivated) bacteria is of extreme importance.

Fluorescence techniques had been used earlier in order to identify and detect bacteria [2], [3], classifying yeast and bacterial cells [4] etc. It has also been shown earlier [1] that measurement of UV induced fluorescence of bacteria (which primarily is due to protein components tryptophan and tyrosine) can be used to determine live and dead bacteria ratio.

This chapter provides a general background to Raman and Fluorescence spectroscopy which are used as major tools in this research. Also a brief background about Principal Component Analysis (PCA) and bacteria is provided.

Fluorescence and synchronous fluorescence spectroscopy

When a molecule absorbs light it is excited to a higher energy state, then it relaxes to the ground state either by dissipating the absorbed energy as heat to the surrounding molecules or by emitting a photon of same or lower energy. This latter process is known as fluorescence.

Bacteria absorb light around 270 nm, the absorbing components (primarily tryptophan and tyrosine) relax to lower energy states by emitting photons or by non-radiative phonon processes. tryptophan emits photons in the 340 nm region and tyrosine emits in the 310 nm region. The overall bacterial fluorescence is mostly due to tryptophan and tyrosine fluorescence.

Fluorescence of tryptophan and tyrosine components in bacteria can be obtained using synchronous fluorescence technique. In the synchronous fluorescence technique, the excitation wavelength is continuously scanned with fluorescence emission being recorded at a fixed separation (in nm) from the excitation wavelength. This can give better resolved fluorescence bands of individual components because different fluorescent components in a sample have different energy separations between their absorption maxima and fluorescence emission maxima.

Thus, by selecting different separation interval between excitation wavelength and emission wavelength, different fluorescent components of a sample can be resolved. For example, in fluorescence of bacteria excited at 270 nm, a broad band is observed with individual components remaining unresolved (Figure 1). However, by choosing a difference of 25-30 nm between excitation and emission wavelength, the fluorescence of tyrosine component can be resolved (Since tyrosine's absorption maxima (280 nm) and emission maxima (310 nm) has a difference of 30 nm) and by keeping difference between excitation and emission wavelength at 65 nm, fluorescence of tryptophan component of the bacteria can be resolved (because tryptophan's absorption maxima (280 nm) and emission maxima (345 nm) has a difference of 65 nm). Figure 1 show *E.coli* fluorescence including tryptophan and tyrosine fluorescence spectra resolved using synchronous fluorescence technique.
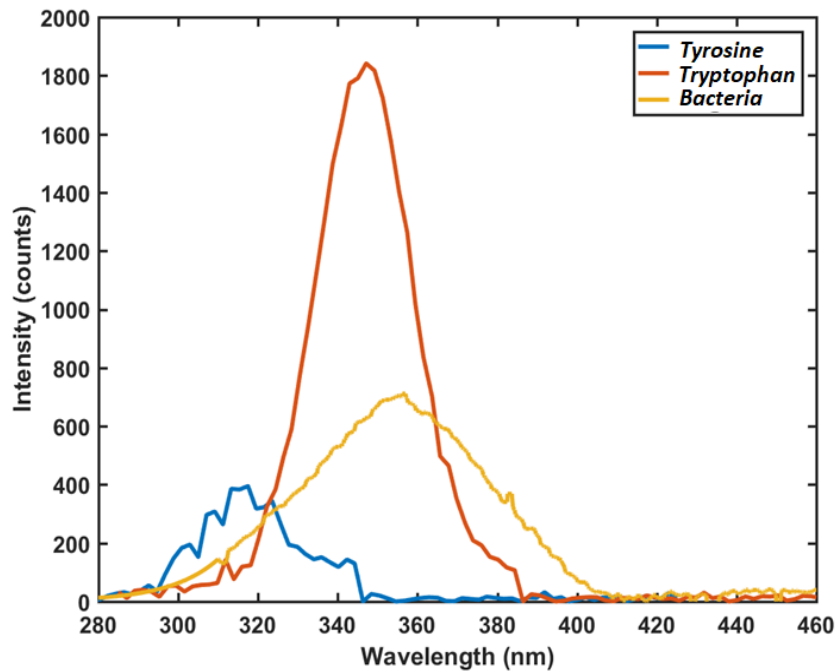
Figure 1. *E.coli* **bacteria fluorescence spectrum with tryptophan and tyrosine components resolved through synchronous fluorescence technique (recorded using handheld instrument developed in this work)**

Principal Component Analysis

Principal Component Analysis (PCA) is a widely used statistical technique for the analysis of data sets consisting of a large number of variables. PCA extracts the most important features from the dataset and represent it along a new set of variables known as principal components [7]. This representation is known as score plot and can be used for classification of unknown datasets into a group of known sets.

Raman Spectroscopy

Raman spectroscopy utilizes Raman Effect, which was discovered by the Indian physicist C.V. Raman. Raman was awarded with the 1930 Nobel Prize for his work. Raman Effect originates from the vibration energy levels of molecular bonds in a material and therefore Raman spectroscopy can be used as a powerful technique to explore underlying molecular bonds in a material. Recently, Raman spectroscopy is becoming very popular for qualitative and quantitative analysis of bio-molecules.

Raman spectroscopy is based on inelastic scattering of light by molecules. Most of the light falling on a molecule is elastically scattered, i.e wavelength of the scattered radiation is same as the incident radiation. This is also known as Rayleigh scattering. However, a very small amount of incident light (roughly 1 in a million photons) undergo inelastic scattering due to exchange of energy between incident photon and vibrating molecular bonds, which means that the wavelength of the scattered radiation is different than the incident radiation. This in-elastically scattered radiation can either be of higher or lower wavelength than the incident radiation. If the in-elastically scattered radiation has a longer wavelength (lower energy) than the incident radiation, it is called stokes scattering and if scattered radiation has a shorter wavelength (higher energy) than the incident radiation, then it is known as anti-stokes scattering. Quantum mechanical probability of anti-stokes wavelength shift is much smaller compared to probability of stokes shift and therefore most of inelastic scattering we observe is stokes shifted.

The origin of Raman Effect lies in the changes in polarizability of a molecule when it interacts with an incoming electromagnetic radiation. This results in formation of new wavelengths of light due to nonlinear effects. A classical mathematical treatment is :

Atoms in a molecular bond vibrate resulting in oscillation of their charges. This charge oscillation can be represented as :

$$\Delta q = q_0 \cos(2\pi f t)$$

Here, q is charge and f is the frequency of vibration of the charge.

Let's represent the electric field of the excitation laser as E, where

$$E = E_0 \cos(2\pi v t)$$

Here, v is frequency of the incident electric field.

This electric field will induce a dipole moment in the molecule, which is given by P, where

$$P = \propto E$$

Where $\propto$ is a material property known as polarizability. $\propto$ can be expanded in a Taylor series expression and can be written as

$$\propto = \propto_0 + \frac{\partial \propto}{\partial q} \Delta q + \cdots$$

Here, $\propto_0$ is the polarizability of the molecule at the equilibrium position,

Then,

$$P = \propto_0 E_0 \cos(2\pi v t) + \frac{\partial \propto}{\partial q} q_0 E_0 \cos(2\pi v t) \cos(2\pi f t)$$

$$P = \propto_0 E_0 \cos(2\pi v t) + \frac{1}{2} \frac{\partial \propto}{\partial q} q_0 E_0 [\cos(2\pi(v + f)t) + \cos(2\pi(v - f)t)]$$

In above equation, the first term is Rayleigh scattering and the second and the third terms are anti-stokes and stokes Raman scattering terms, respectively. It can be noticed that the Raman scattering terms can exist only when the $\frac{\partial \propto}{\partial q}$ term is non-zero.

7

Although correctly predicting Raman Effect, this simple classical treatment fails to predict correct intensities of stokes and anti-stokes Raman lines. For that purpose, we need to do analysis of Raman scattering according to quantum mechanical theory. According to quantum mechanics, factor $e^{hv/kT}$ gives the ratio of molecules in ground energy state and any particular higher energy state of energy hv. Since anti-stokes Raman lines can come only from molecules in higher energy states, therefore ratio of stokes and anti-stokes lines can be roughly represented by the following formula,

$$\frac{I stokes}{I anti - stokes} = e^{hv/kT}$$

Here, k is Boltzmann's constant and T is temperature in Kelvin and hv is quantum energy gap between ground energy state and higher vibration energy states. At room temperature under normal circumstances $e^{hv/kT} \gg 1$, therefore compared to ground energy state, higher energy states will have relatively very few molecules. This will result in much weaker intensities of anti-stokes Raman lines compared to stokes lines.

Figure 2 (A) shows quantum mechanical picture of Raman scattering. Figure 2 (B) shows a simplified block diagram of a Raman spectrometer and 2 (C) shows a typical Raman spectrum of *E.coli* bacteria after baseline removal. Prominent bands in the figure are marked. A detailed assignment of Raman bands to the corresponding bond vibrations and molecular origin are given in Appendix B.
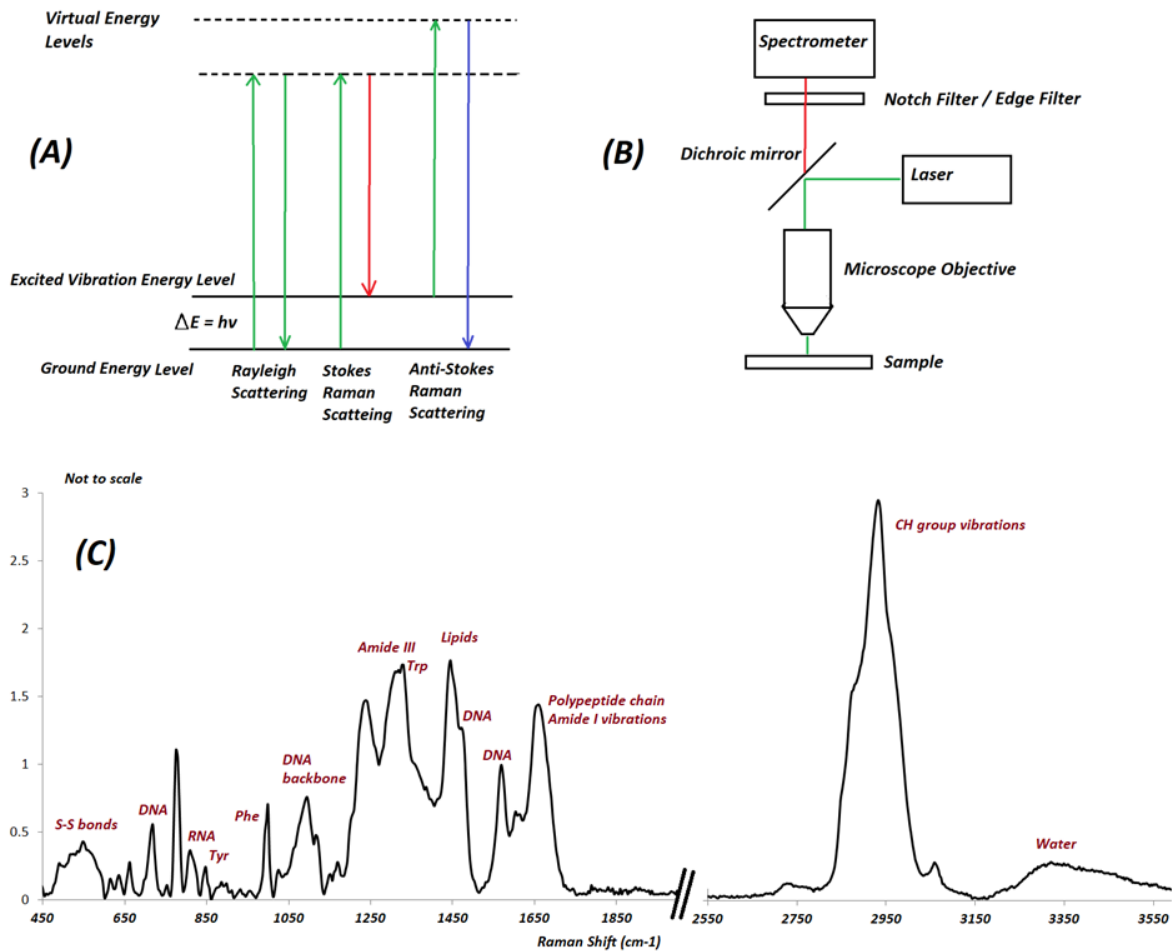
Figure 2. (A) Quantum mechanical description of Raman effect; (B) Block diagram of a Raman spectrometer (C) Typical Raman spectrum of *E.coli* with bands marked (Phe : Phenylalanine, Tyr : tyrosine, Trp : tryptophan)

Bacteria and ultraviolet light

Bacteria are single cell microorganisms found ubiquitously in nature. Bacteria are one of the first forms of life evolved on earth and are present from deep below in earth's crust to the boundaries of earth's atmosphere and space [8],[9],[10]. Bacteria can survive in extreme harsh conditions. Also in human body, bacterial cells outnumber human body cells. A large number of bacterial species are benign and necessary to humans; however there are also bacteria which are

9

extremely dangerous to human health. Many of the wound infections are caused by bacteria. Waterborne bacteria are often a cause of many widespread diseases in developing and under-developed areas of the world.

Bacteria cells have a cell wall and cell membrane which act as an outer protective layer for the internal components such as DNA. Composition of an average *E. coli* cell is given in the Table 1 [11].

Component	Dry Weight %
Proteins	55
RNA	20.5
DNA	3.1
Lipids	9.1
Lipo-polysaccharide	3.4
Peptidoglycan	2.5
Glycogen	2.5
Polyamines	0.4
Metabolites, cofactors & ions	3.5

Table 1. Composition of *E.coli* bacteria by dry weight (adapted from [11])

All of the major components of a bacterial cell (proteins, DNA, and RNA etc.) absorb light in the ultraviolet region of electromagnetic spectrum. Proteins have absorption intensity maxima at 280 nm and DNA/RNA have an absorption maxima around 260 nm. A bacterial cell

shows absorption maximum at around 270 nm. Figure 3 shows a typical absorption spectrum of *E. coli* cells in water.
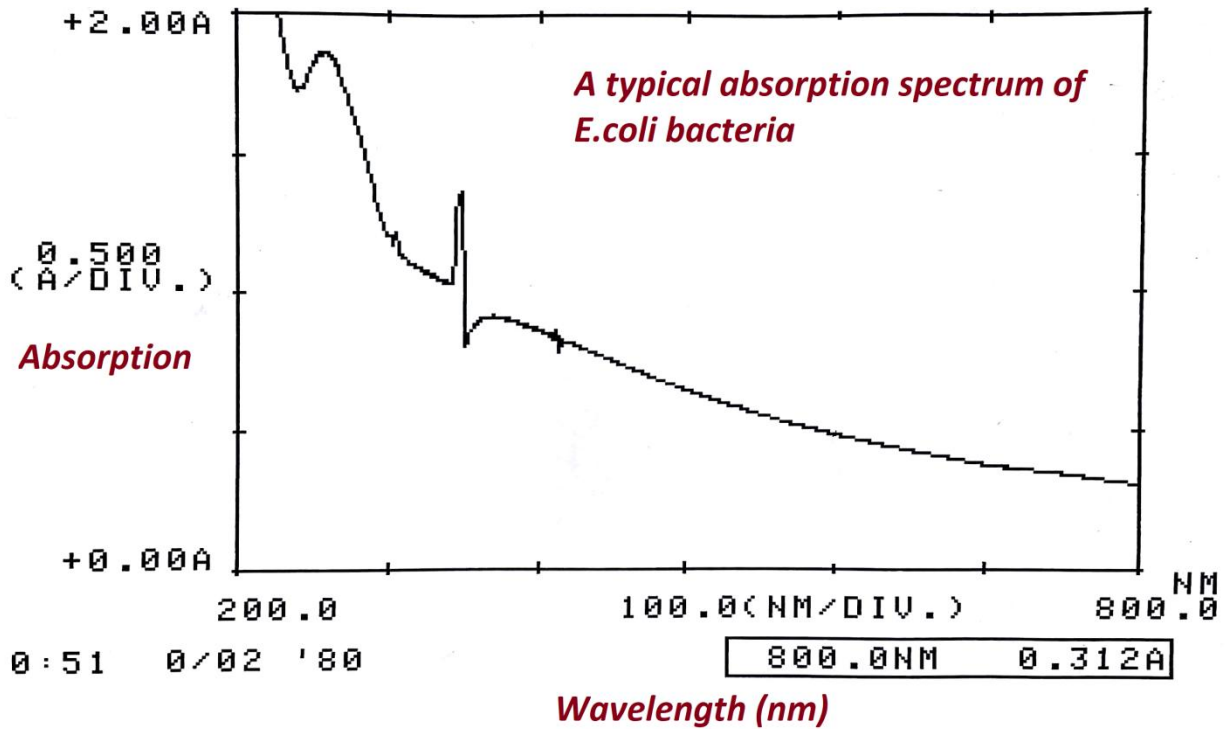
Figure 3. *E.coli* **Absorption Spectrum**

As bacteria absorb ultraviolet light, they undergo chemical changes resulting in damage to absorbing components, tryptophan, tyrosine, DNA and RNA; leading to death (inactivation) of bacterial cell. It is well established that absorption of Ultraviolet light by DNA results in formation of several photoproducts, primarily of pyrimidine bases [12]. Of these photoproducts, Thymine cyclo-butane dimers are shown to be the most abundant, where two adjacent thymine bases connect with each other forming a Thymine dimer. Because of such damage to DNA, a bacterial cell is unable to replicate. This results in the inactivation of the bacteria.

CHAPTER III

HANDHELD INSTRUMENT DESIGN AND CONSTRUCTION

There is a critical need of fast, in-situ determination of live and dead bacteria in order to control diseases due to bacterial infections. It has been shown in earlier in [1] that tryptophan and tyrosine fluorescence can be used to determine live and dead bacteria. Based on this concept, a handheld instrument was designed and constructed which can record fluorescence of bacteria, coming from tryptophan and tyrosine. This device was designed in order to be used in the field for fast (minutes), in-situ determination of live and dead bacteria. In the future, Raman capability will also be incorporated in this device. This section describes the design and construction of this device.

Block diagram

The handheld device consists of an excitation monochromator, an emission monochromator, a display and control unit, UV LEDs and a UV sensitive camera. A block diagram of this device is shown in Figure 4.
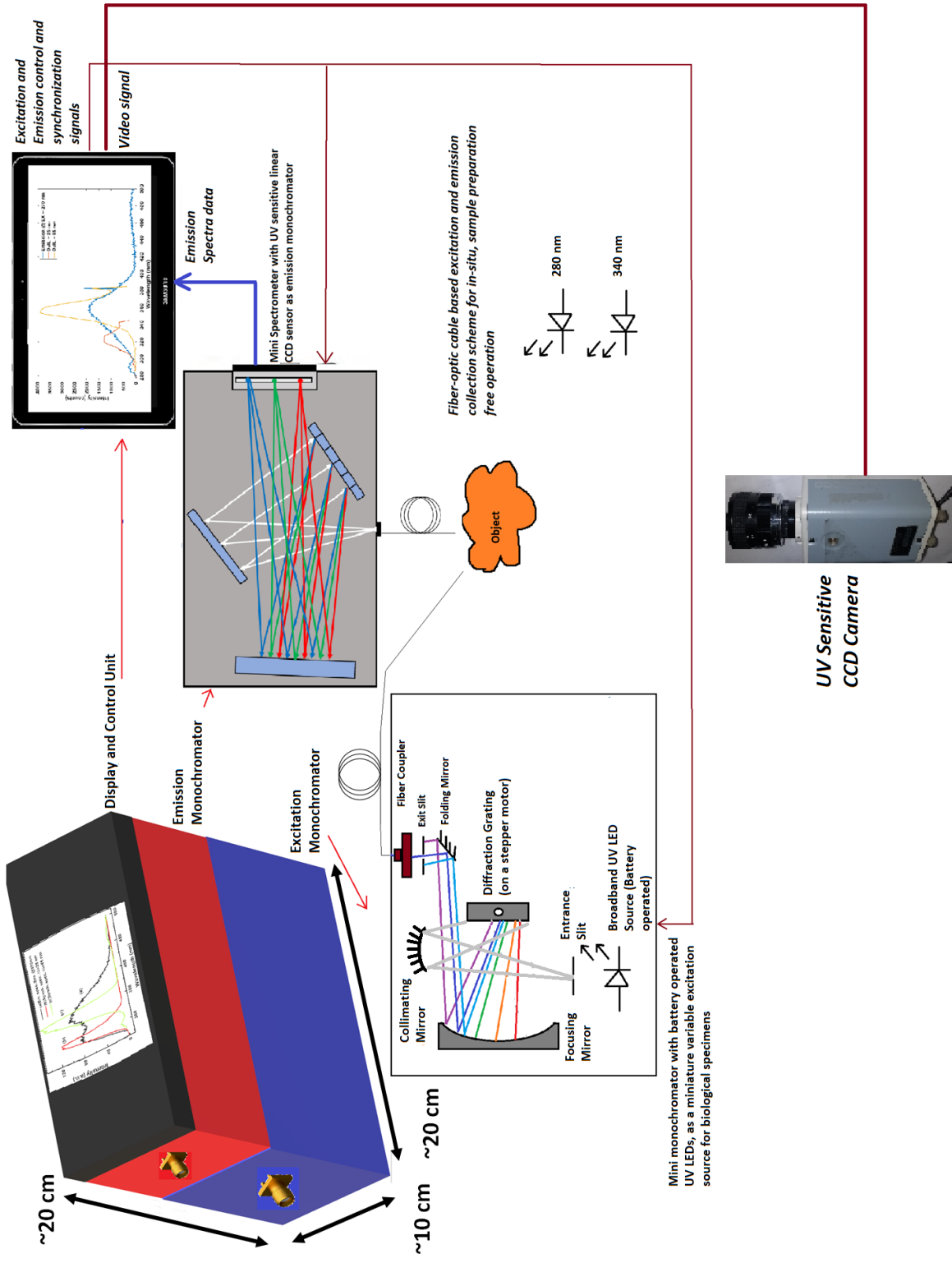
Figure 4. Handheld device block diagram

Excitation and Emission control and synchronization signals

Video signal

Emission Spectra data

Mini Spectrometer with UV sensitive linear CCD sensor as emission monochromator

Fiber-optic cable based excitation and emission collection scheme for in-situ, sample preparation free operation

280 nm

340 nm

UV Sensitive CCD Camera

Object

Display and Control Unit

Emission Monochromator

Excitation Monochromator

~20 cm

~20 cm

~10 cm

Fiber Coupler

Exit Slit

Folding Mirror

Diffraction Grating (on a stepper motor)

Entrance Slit

Broadband UV LED Source (Battery operated)

Collimating Mirror

Focusing Mirror

Mini monochromator with battery operated UV LEDs, as a miniature variable excitation source for biological specimens

The emission monochromator which is integrated with a linear CCD detector acts as the fluorescence measurement unit. Excitation monochromator scans the excitation wavelength of the light required for normal and synchronous fluorescence measurements. Fused silica optical fibers capable of transmitting UV light are used for excitation, as well as collection of the sample fluorescence emitted. Fixed wavelength UV LEDs are used for bacterial inactivation as well as excitation of fluorescence (excited at a fixed wavelength). A UV and visible wavelength sensitive CCD camera is also integrated with this device in order to assist in proper pointing of optical fibers for spectra acquisition. Current Display and control unit is a compact laptop which is used for entering the commands, display and recording of the spectra from the emission spectrometer.

Emission monochromator/spectrometer

The emission monochromator component is used to record the fluorescence emitted from bacteria. The currently used emission monochromator utilizes a Czerny-Turner configuration. Spectrometer optical bench was obtained from B&W-Tek and custom made optical components were used to assure sensitivity in UV region. The detector is Sony ILX511B, consisting of a linear array of 2048 pixels. The detector pixels were coated with (lumogen violet 570) which converts ultraviolet light into visible light, which improves the sensitivity in ultraviolet region of the spectrum, owing to the higher quantum efficiency of the detector in the visible wavelengths. The diffraction grating was obtained from the Newport Corp, was a ruled grating with 1200 lines/mm and having more than 70 percent efficiency in the ultraviolet region. Figure 5 shows details of the emission monochromator/spectrometer.
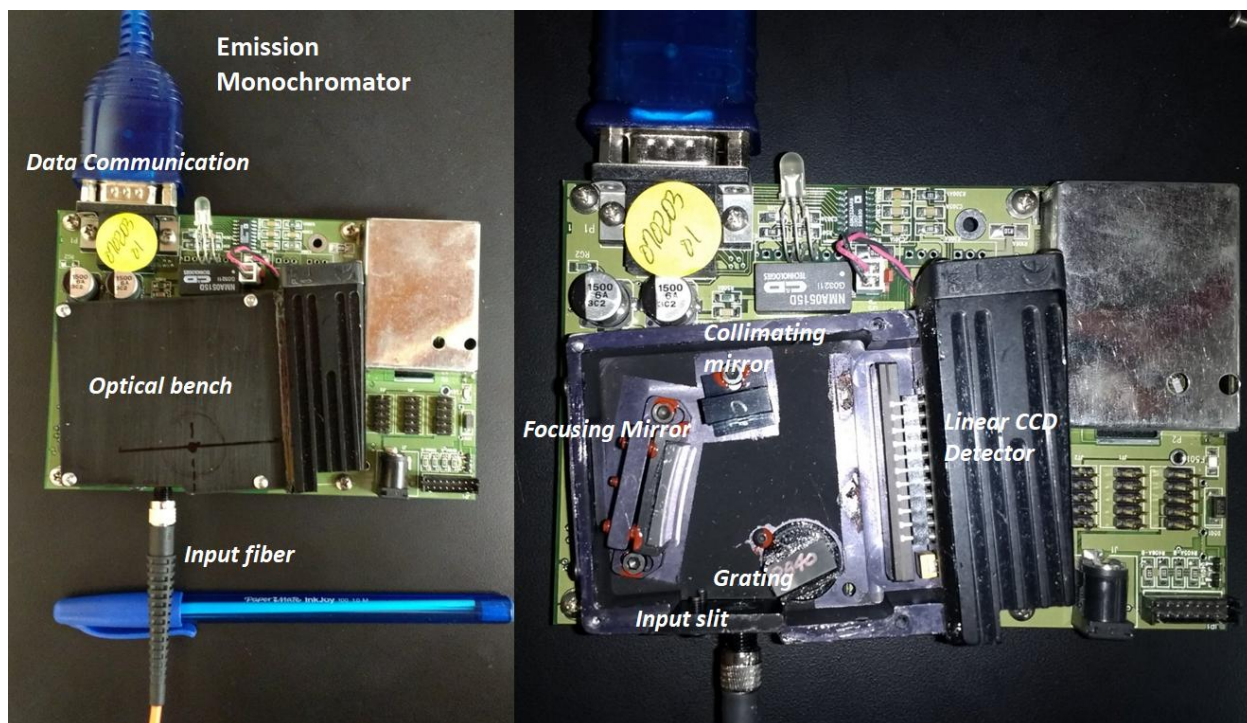
Figure 5. Internal configuration of emission monochromator

Excitation monochromator / excitation LEDs

The excitation monochromator has an optical arrangement similar to that of emission monochromator, it consists of an input slit, a collimating mirror, a focusing mirror and a diffraction grating. The diffraction grating is mounted on a stepper motor (8HS11-0204S), rotation of this motor is controlled by an arduino micro-controller. The light from the focusing mirror is passed through an exit slit to deliver a monochromatic beam. A series of LEDs emitting in the wavelength range of 265 nm to 315 nm acts as light source for the excitation monochromator which is currently constructed. The experimental system has been tested for synchronous measurements using an external monochromator, the results are shown in chapter V. There are also two LEDs (275 nm and 340 nm) in this device which can be used for excitation of protein fluorescence and protein photoproducts fluorescence. These LEDs were obtained from Vishay Semiconductors (275 nm) and Marktech Optoelectronics (340 nm). The 275 nm LED can

15

serve dual functions, fluorescence measurements as well as bacteria inactivation. Figure 6 show internal arrangement of excitation monochromator.
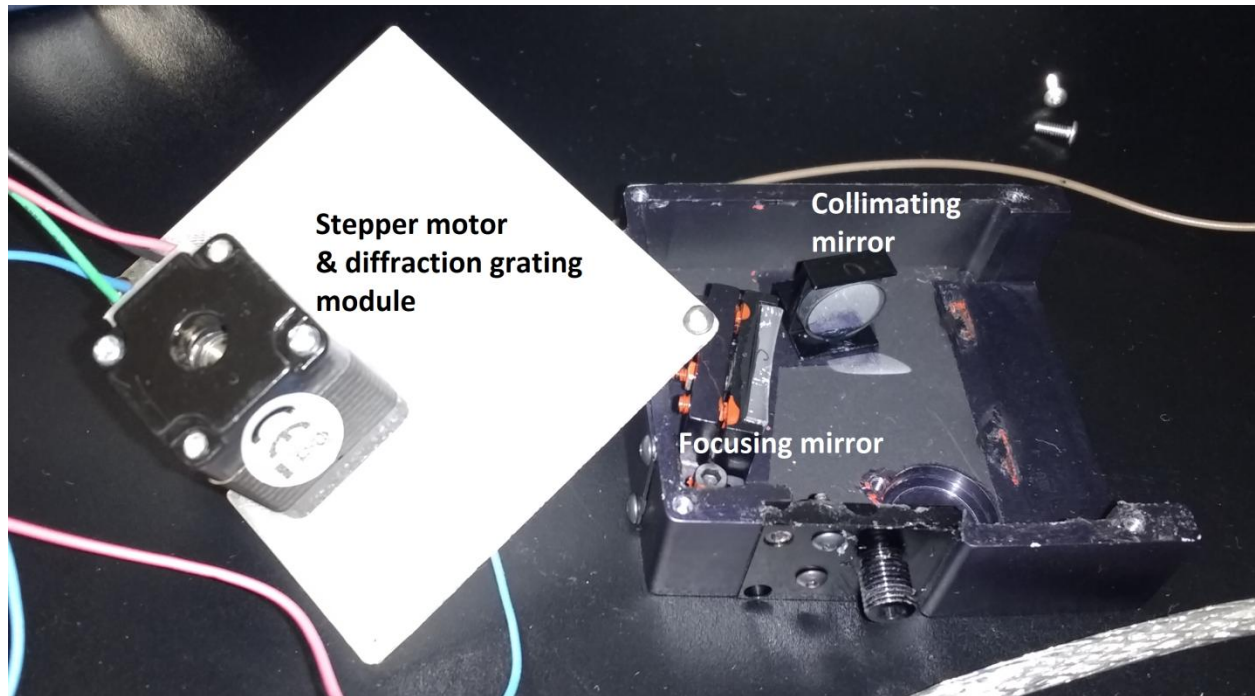
Figure 6. Excitation monochromator internal configuration

Display and control unit

The current display and control unit is a compact laptop computer which runs custom software based on MATLAB environment which consists of a Graphical User Interface (GUI) that allows for selection of the parameters for synchronous spectra display as well as for Principal Component Analysis of the recorded data.

UV sensitive CCD camera

In order to properly point the fluorescence excitation and emission probe or fiber, it is necessary to find out where in the wound bacteria are present. For this purpose a camera is

designed which is sensitive to ultraviolet light (340 nm -390 nm) region. This camera can detect the fluorescence from tryptophan when tryptophan is excited by UVC LED. By looking at the images, it could be determined where bacteria are present and where the collection fiber should be pointed.

The imaging camera used for this purpose is a black & white CCD camera. This camera does not have UV cut filter which opens up its sensitivity to the near UV region. Also, this camera has a monochrome (black & white) sensor without the bayer filter mask (used in color cameras). Lack of Bayer filter mask give designed camera better sensitivity to near UV radiation. In front of camera, a UV pass and visible block filter is placed. Transmission characteristics of this filter are shown in Figure 7.
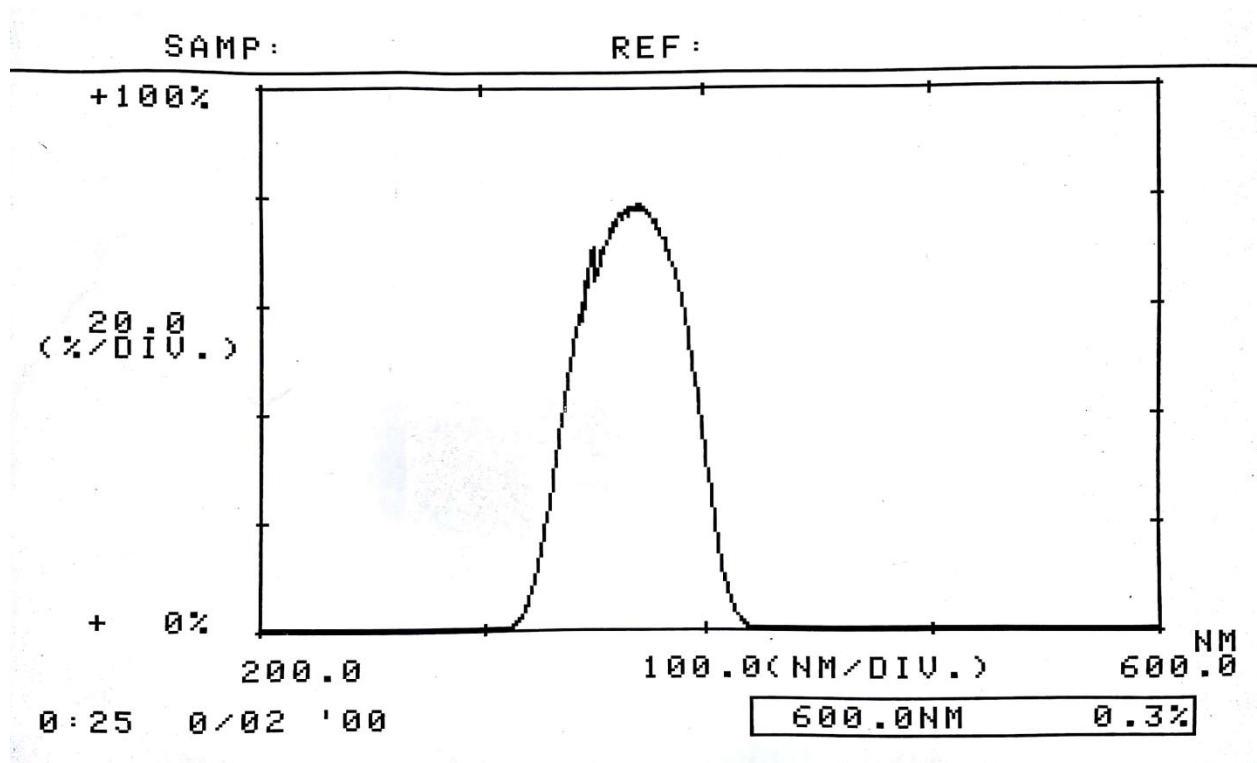
Figure 7. Transmission characteristics of the UV pass filter used in CCD camera

CHAPTER IV

MATERIAL AND METHODS

Bacterial culture preparation

      Escherichia coli (*E. coli*) (strain K-12, GM1655) was obtained from the Bacteriological Epidemiology and Antimicrobial Resistance unit, USDA-ARS. Bacteria were cultured on Tryptic Soy Agar (TSA) plate at 37^oC, then was subcultured to 10 ml of Luria Bertani (LB) growth medium and incubated overnight at 37^oC in a water bath. Bacteria were harvested in stationary phase of growth by centrifugation at 3300 rpm for 5 minutes. The bacterial pellet was washed three times with 0.9%, w/v, saline solution to get rid of the growth media. Then the pellet was diluted in saline to a concentration of roughly ~ 10^8 cells/ml by measuring optical density of the solution at 600 nm (OD600 ~ 0.1, measured using Shimadzu UV160 spectrophotometer). *Bacillus Thuringiensis* bacteria were grown from their spores for the experiments.

UV irradiation of bacteria using mercury lamp

      A mercury lamp (Oriel model no. 66002) was used for UV irradiation. Output of mercury vapor lamp was passed through a filter which blocks the visible region of the spectrum and allows only the ultraviolet region of the spectrum (250 nm to 380 nm) to pass through it (Figure 8). The resultant output spectrum of the mercury vapor lamp was measured by Jarrell Ash monochromator using a Hamamatsu PMT (Photomultiplier Tube model R928) as detector (Figure 9).

Figure 8. UV Pass Filter Transmission Spectra

Figure 9. Resultant output spectrum of Mercury vapor lamp after passing through UV pass filter

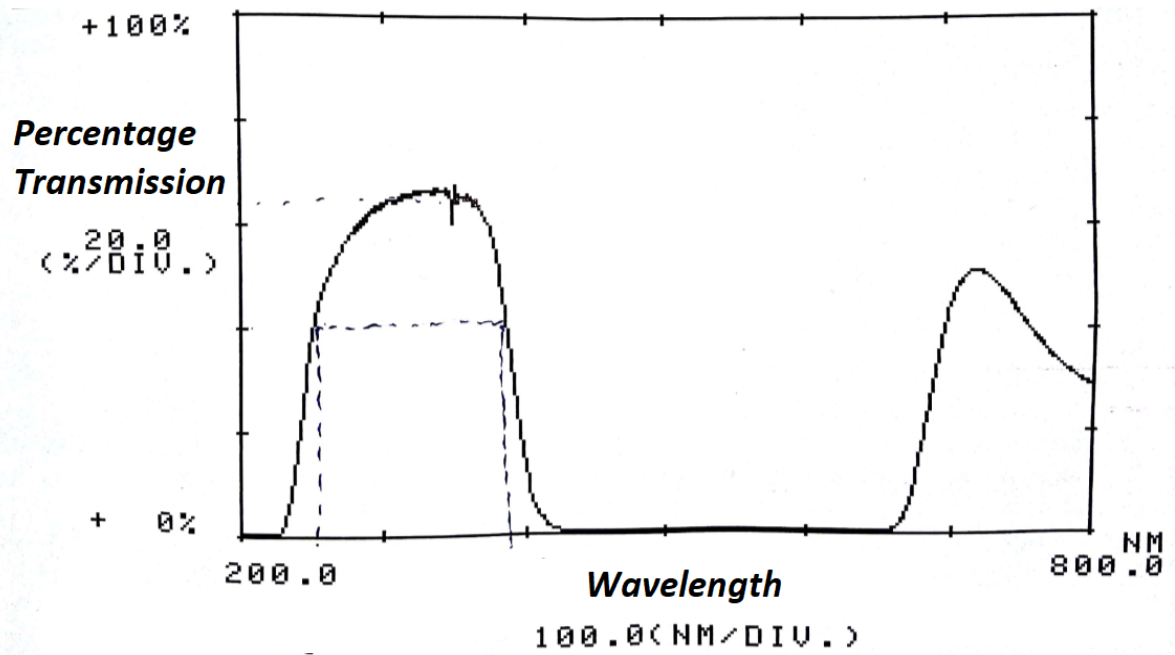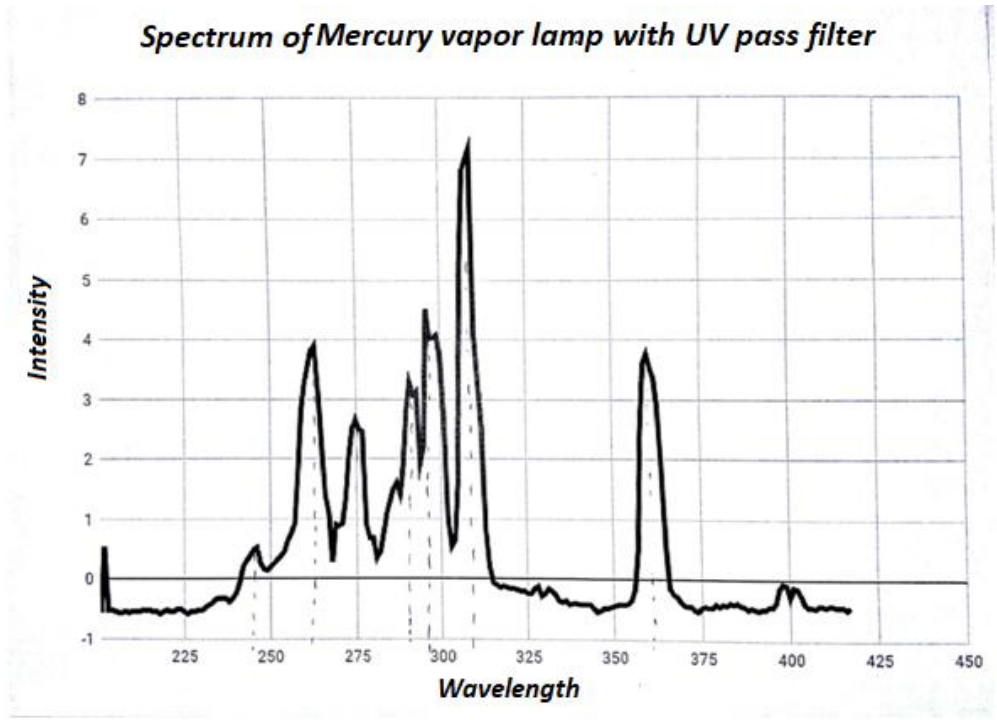A Molectron detector (PM3Q with EPM1000) was used to measure ultraviolet irradiation intensity. The UV intensity was adjusted to be roughly 2 mW/cm^2 for bacterial irradiation. Bacterial solutions were irradiated using different doses. UV Dose is the product of UV light intensity and time and is calculated using the following parameters:

Dose = Intensity x Time= millijoules/(sec)(cm2) x time= mJ/cm2

Nine ml of bacterial solution was irradiated at period betweeen 10 and 20 minutes to obtain doses of 1200 mJ/cm2 and 2400 mJ/cm2. After irradiation, bacterial culture was concentrated by centrifugation at 3300 rpm (Fisher Scientific Centrific Model 228) for 5 minutes, the supernatant was discarded and the bacterial pellets was re-suspended in 100 micro-liters of saline. A 2.5 micro-liter of bacterial solution was put on an aluminum mirror or a single crystal silicon cuvette for Raman spectra acquisition.

UV irradiation of bacteria using 280 nm UV LED

Since mercury lamps require a bulky power supply, are environmentally hazardous and expensive compared to LEDs, therefore UVC LEDs can be a very attractive alternative to mercury lamps for bacterial inactivation. UVC LEDs are very compact, energy efficient and can be operated with tiny batteries which eliminate the need of a bulky power supply. Using these LEDs can also make UV bacterial inactivation easier to be carried out in-situ and in field using the handheld spectrometer instrument.

UVC LEDs (Vishay Semiconductor VLMU60CL00-280-125) emitting light in ultraviolet region with maximum emission at 280 nm were used for UV irradiation of bacterial solution. This particular LED was chosen because it has three times more optical power output compared to other LEDs available at slightly lower wavelengths. This UVC LED has a FWHM (Full Width

at Half Maxima) band-width of 10 nm. The output light from this LED was collimated with two lens combination. The emission spectrum of this LED obtained from its datasheet was shown in Figure 9. 1.5 ml of bacterial solution (OD600 ~ 0.5) was irradiated with LED, the final intensity falling on the quartz cuvette containing bacterial solution was roughly set to 0.2 mW/cm2 (measured using Hamamatsu S1336-8BQ UV detector) and the exposure times were 30, 60, 90, 120, 150, 180 and 210 minutes.
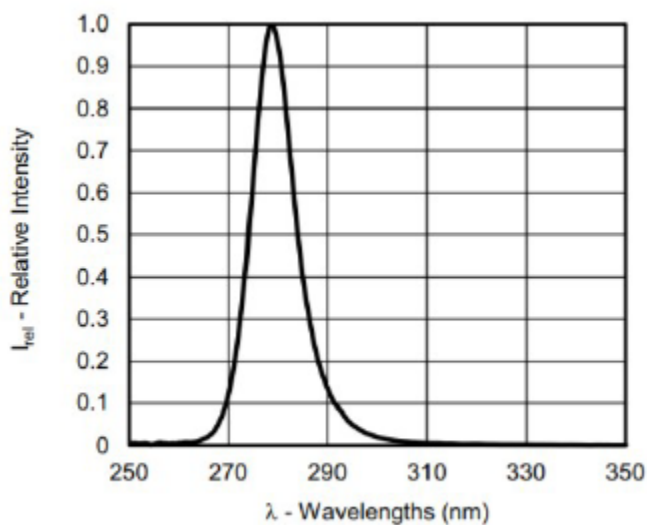
Figure 10. UVC LED emission spectrum

Raman spectra acquisition

Raman spectra from bacteria samples were recorded in wet and dry conditions using Horiba Xplora plus Raman microscope. In the wet condition, spectra were recorded immediately after the bacteria were put on the mirror / single crystal silicon cuvette well using 10X microscope objective. Excitation wavelength was 638 nm and laser power was 25 mW. Spectrum acquisition time was 100 seconds and was acquired repeatedly 9 times, and results were averaged.

In the dry condition, spectra were recorded immediately after the bacterial solution had dried on the aluminum mirror/ single crystal silicon cuvette. In this condition, it was possible to use 100X microscope objective and the obtained spectra were much better resolved. Excitation laser wavelength was 638 nm and power was 25mW. In order to obtain representative spectra of bacterial cells in dry condition, spectra acquisition was done at six different points on the sample. For every point, the spectrum acquisition time was 100 seconds and 3 spectra were accumulated, and results were averaged.

Bacterial cells were examined under the microscope to observe any damage due to Raman laser, no such damage was observed. The temperature at the laser focus point was measured with two different thermocouple temperature sensors by focusing directly the Raman excitation beam on the temperature sensor, the maximum temperature increase observed was from 23 degree Celsius (ambient room temperature) to 35 degree Celsius.

Bacteria Plating for CFU Counting

Bacteria CFU (Colony Forming Units) counting was done by taking 100 micro-liters of the bacteria solution, serially diluting it and then plating it on agar plates. Plated agar plates were kept in an incubator for 24 hours for bacteria growth and colonies were counted afterwards to estimate CFU counts. CFU counting was performed before UV irradiation and after different doses of UV irradiation.

Principal Component Analysis

Principal Component Analysis (PCA) was performed on set of Raman data acquired for *E.coli* subjected to different UV doses using MATLAB software package. Six spectra were

acquired from each sample subjected to different UV doses. Baseline was removed using a standard procedure described in Appendix I and spectra were normalized with respect to lipid peak at 1450 cm-1, then were subjected to PCA analysis.

Determination of Thymine dimers in Raman spectra

Thymine dimers were made from Thymine as per procedure described in [17]. Thymine solution was irradiated with UV LED in frozen condition and formation of Thymine dimers was monitored by observing the complete disappearance of the 260 nm band in absorption spectrum of the irradiated solution. Raman spectra of Thymine and Thymine dimers were recorded with the same setup as described earlier in this chapter. The excitation laser wavelength was 638 nm and power was 25mW. Spectra were taken at six different points of dried Thymine and Thymine dimers in order to obtain a representative spectrum. 10X microscope objective was used, spectrum acquisition time was 100 seconds and was acquired repeatedly 3 times, and results were averaged.

Protein solution preparation

In order to study UV irradiation effect on proteins, ovalbumin protein solution was prepared to a final concentration of 0.4 mg/ml in distilled water. Ovalbumin protein used in experiments was provided by Dr. Maria King. Protein solution was irradiated with mercury vapor lamp as per the arrangement described earlier in this chapter. 3 ml of protein solution was put in a quartz cuvette and irradiated with the mercury vapor lamp. After irradiation a 2.5 micro-liter protein solution was put on an aluminum mirror for Raman spectra acquisition. Raman

spectra acquisition of protein samples was carried out with the same setup and parameters as described earlier in this chapter for dry condition.

Fluorescence spectra acquisition

In addition to using our handheld instrument, fluorescence and synchronous fluorescence spectra were also recorded using Shimadzu RF-5301PC spectrofluorophotometer for bacteria and protein samples. Fluorescence and synchronous fluorescence measurements were recorded using three ml of bacteria/protein solution placed in a quartz cuvette of 1cm path length.

CHAPTER V

RESULTS AND DISCUSSION

Handheld spectrometer recorded data

E.coli bacterial cells were prepared by the procedure described in chapter IV. The bacterial solution concentration used in the experiments was approximately 4 X 10^8 cells /ml (OD 600 ~ 0.5). This solution was irradiated with mercury lamp with UV pass filter as per the procedure described in chapter IV. For fluorescence excitation, UVC LED (280 nm) from Vishay semiconductors (VLMU60CL-280-125) was used. Emission spectra were collected and were then subjected to Principal Component Analysis (PCA). Results are shown in Figure 11 and 12.
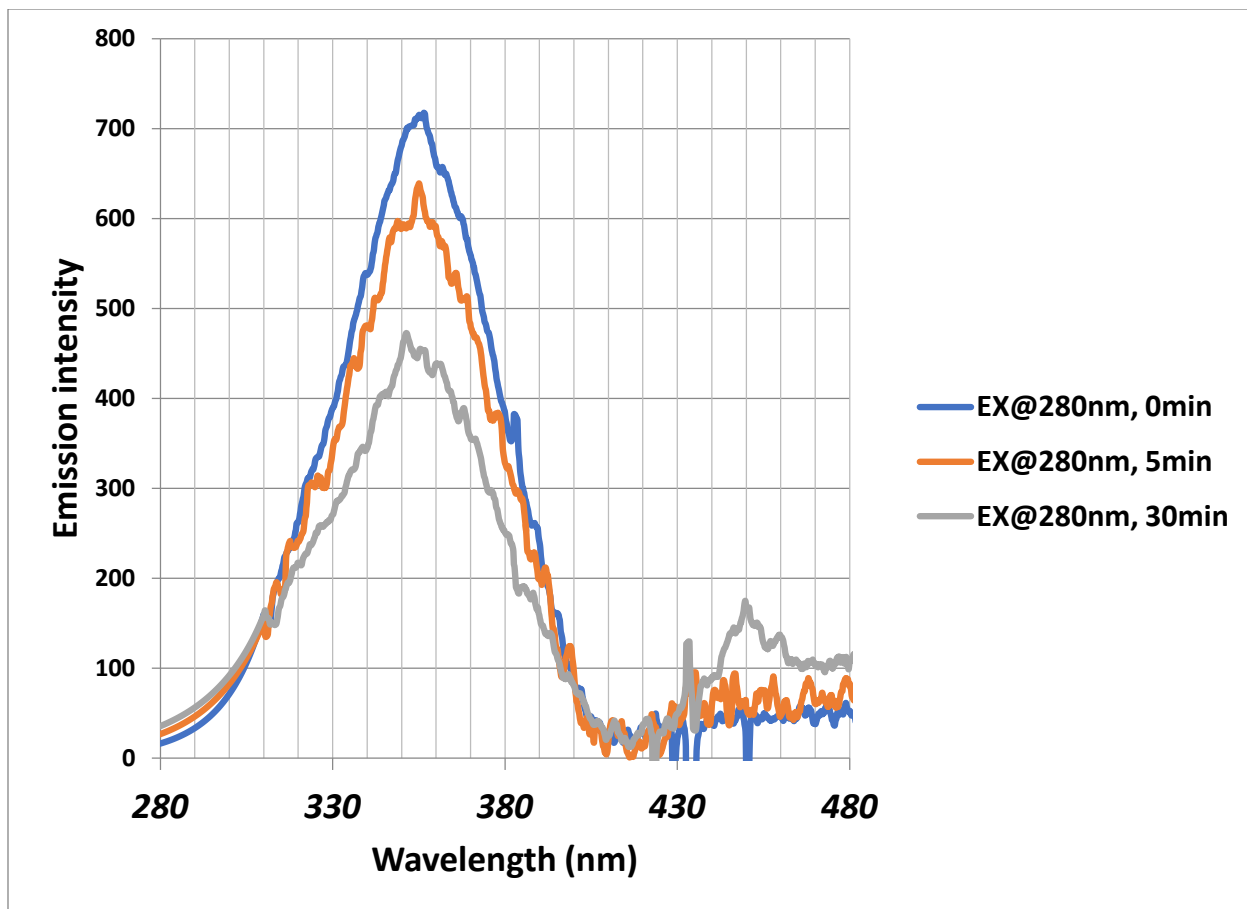
Figure 11. Emission spectrum from *E.coli* with UV irradiation time (7 mW/cm2 with mercury vapor lamp). For fluorescence spectra recording, samples were excited with 280 nm LED.
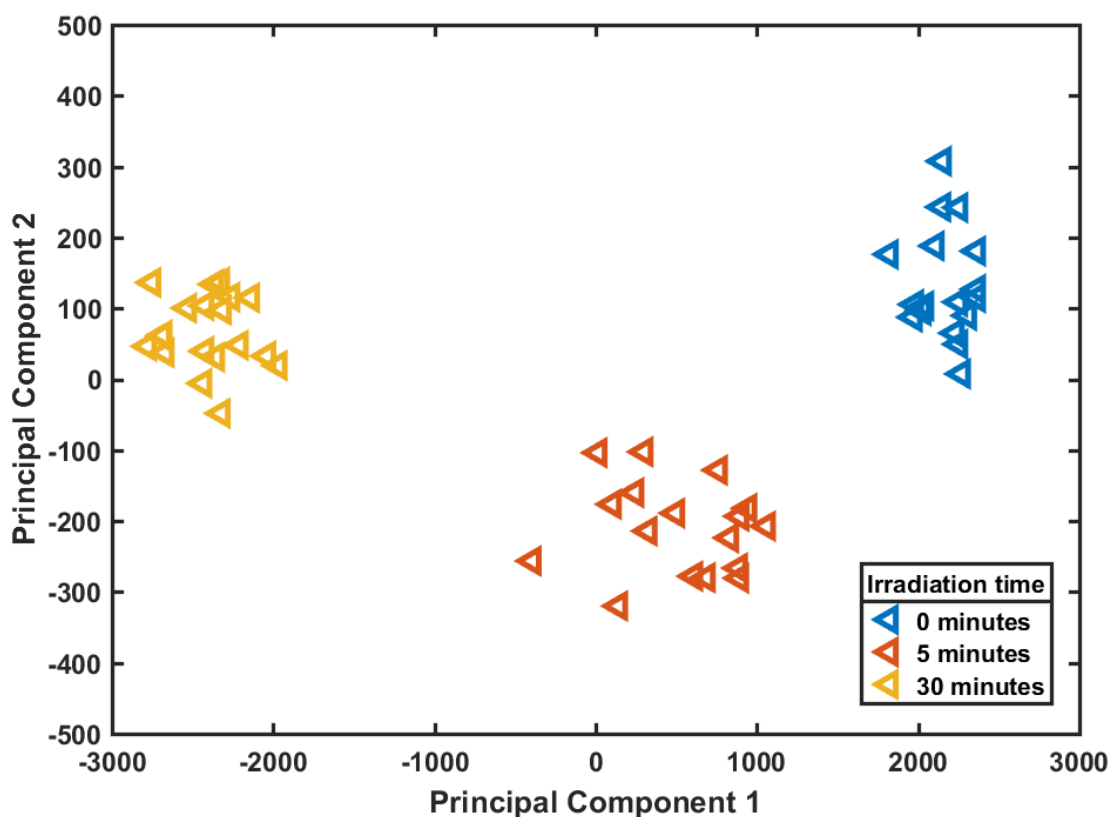
Figure 12. PCA Score plot for emission spectrum from *E.coli* with UV irradiation time (7 mW/cm2 with mercury vapor lamp). For fluorescence spectra recording, samples were excited with 280 nm LED

Figure 13 shows the three dimensional view of Excitation-Emission Matrix (EEM) of *E.coli* bacteria (concentration ~ 10 ^8 cells/ml), as recorded from the handheld instrument and custom MATLAB software. For scanning the excitation wavelengths, an external monochromator was paired with the current instrument. Recording and plotting of this entire three dimensional EEM took no more than 5 minutes.

After recording three dimensional EEMs for every UV radiation time, synchronous fluorescence spectra for $\Delta\lambda = 65\ nm$ and $\Delta\lambda = 25\ nm$ which corresponds to tryptophan and tyrosine, respectively were computed in software and compared (Figure 14). Computation of

these synchronous fluorescence spectra from 3D EEM takes just a few seconds. Figure 15 shows

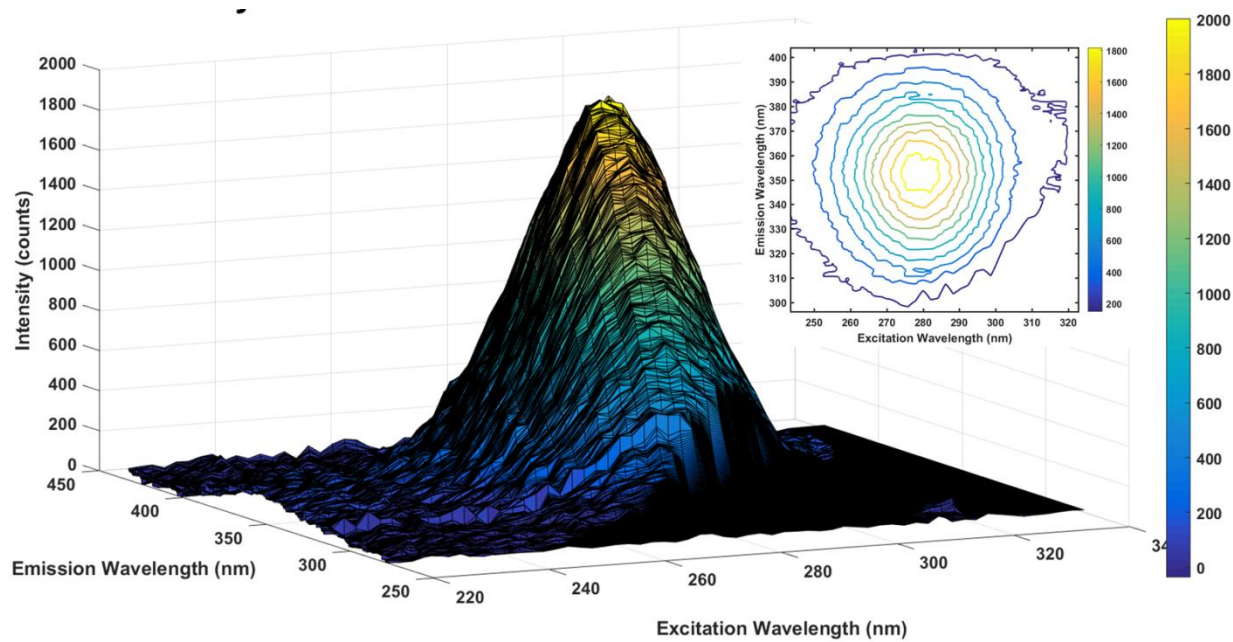a picture of the handheld device.

Figure 13. 3D visualization of EEM for *E.coli* (concentration ~ 10^8 cells /ml). *Inset:* 2D projection of EEM
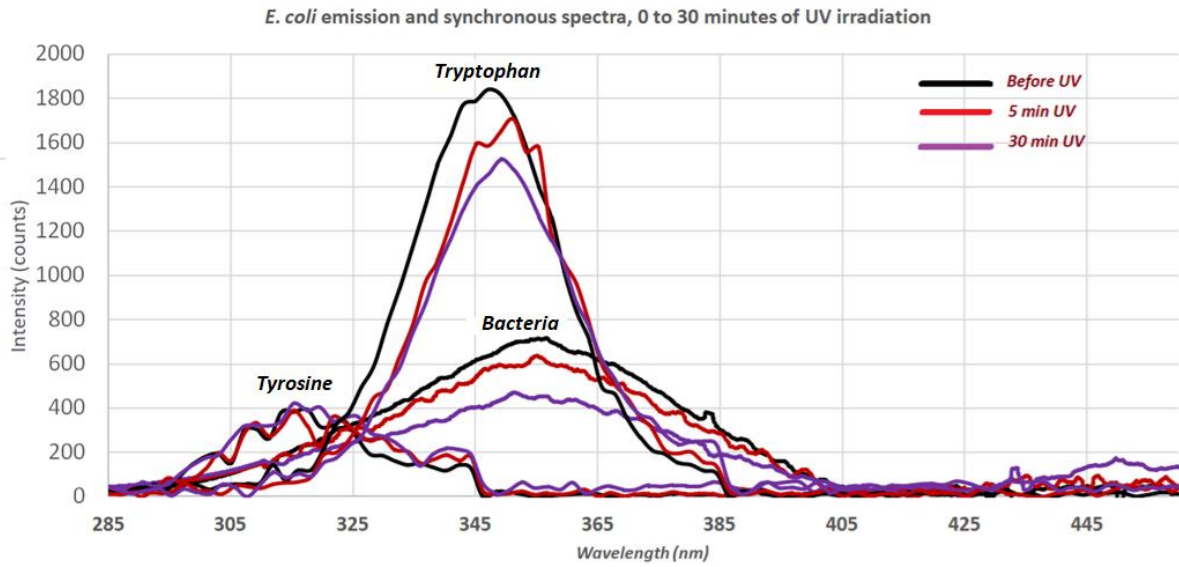
Figure 14. Emission and synchronous spectra of *E.coli* bacteria recorded with developed handheld device. tyrosine and tryptophan components were obtained with synchronous fluorescence recording with delta lambda of 25 nm and 65 nm respectively
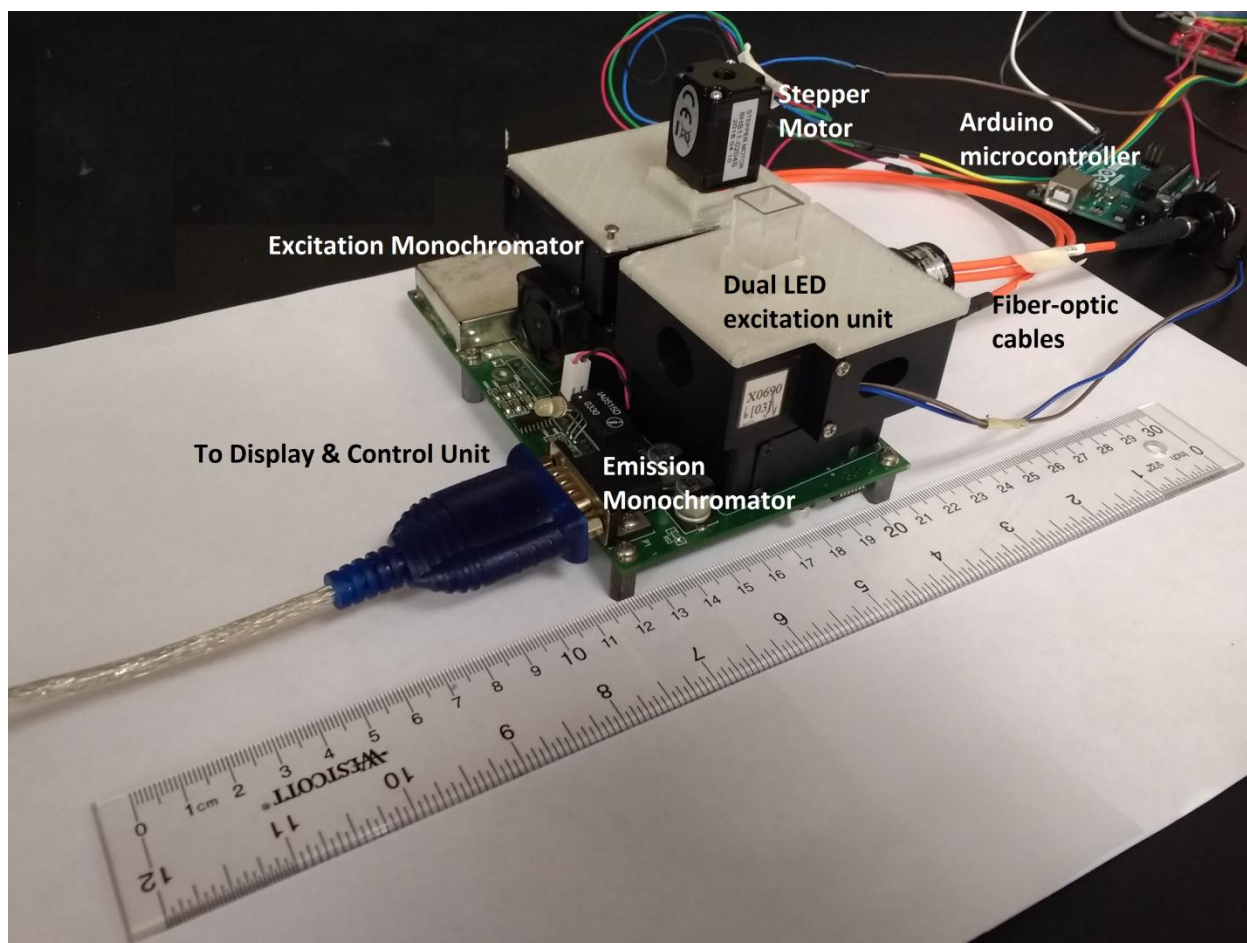
Figure 15. Handheld device

Effect of UV irradiation on bacterial cells studied through Raman spectroscopy

The Raman spectrometer was used to study the effect of UV radiation on bacteria before and after UV radiation. The spectra of bacteria in wet condition are presented in Figure 16. After UV irradiation for 10 minutes, a higher band around 1400 cm-1 was detected. This band increased after longer UV irradiation for 20 minutes.

Spectra of bacteria recorded in dry condition are shown in Figure 17. Better resolved bands were detected from bacteria in dry condition than bacteria in wet condition. The baseline was removed using a standard procedure described in Appendix A and the spectra were

30

normalized with respect to the lipid peak at 1450 cm-1 (Figure 18). In these spectra, a rising band around 1410 cm-1 was detected after the bacteria were exposed to UV irradiation for 10 minutes. This band was increased as duration of UV exposure was increased. It is presumed that the 1400 cm-1 band in wet condition and the 1410cm-1 band in dry condition are the same UV induced photoproducts. The observed red shift of 10cm-1 and broadening of the 1410 cm-1 band might be due to change in local environment around the bacteria molecules in wet and dry conditions.

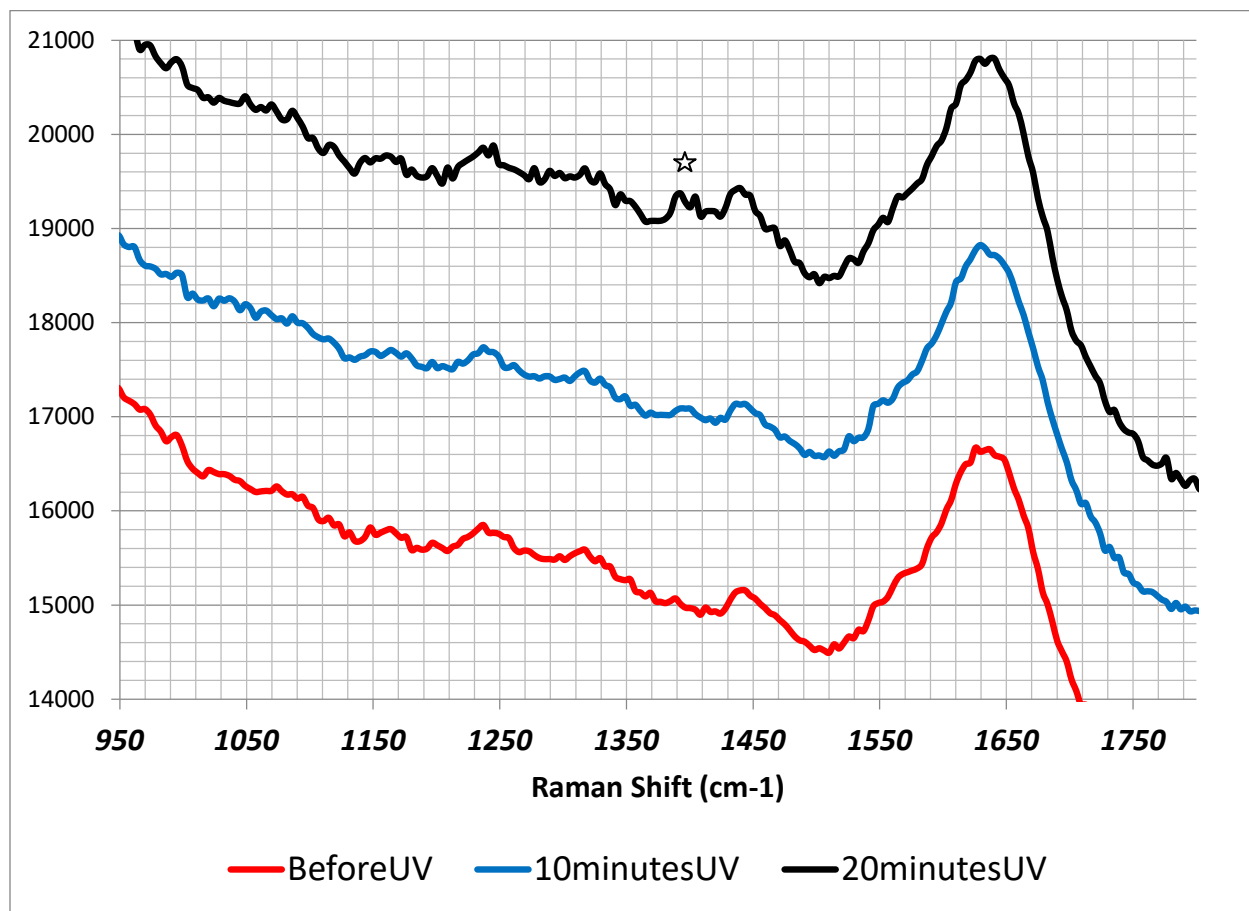**Figure 16. Raman spectra of *E.coli* in wet condition before and after UV radiation at 10 and 20 minutes**
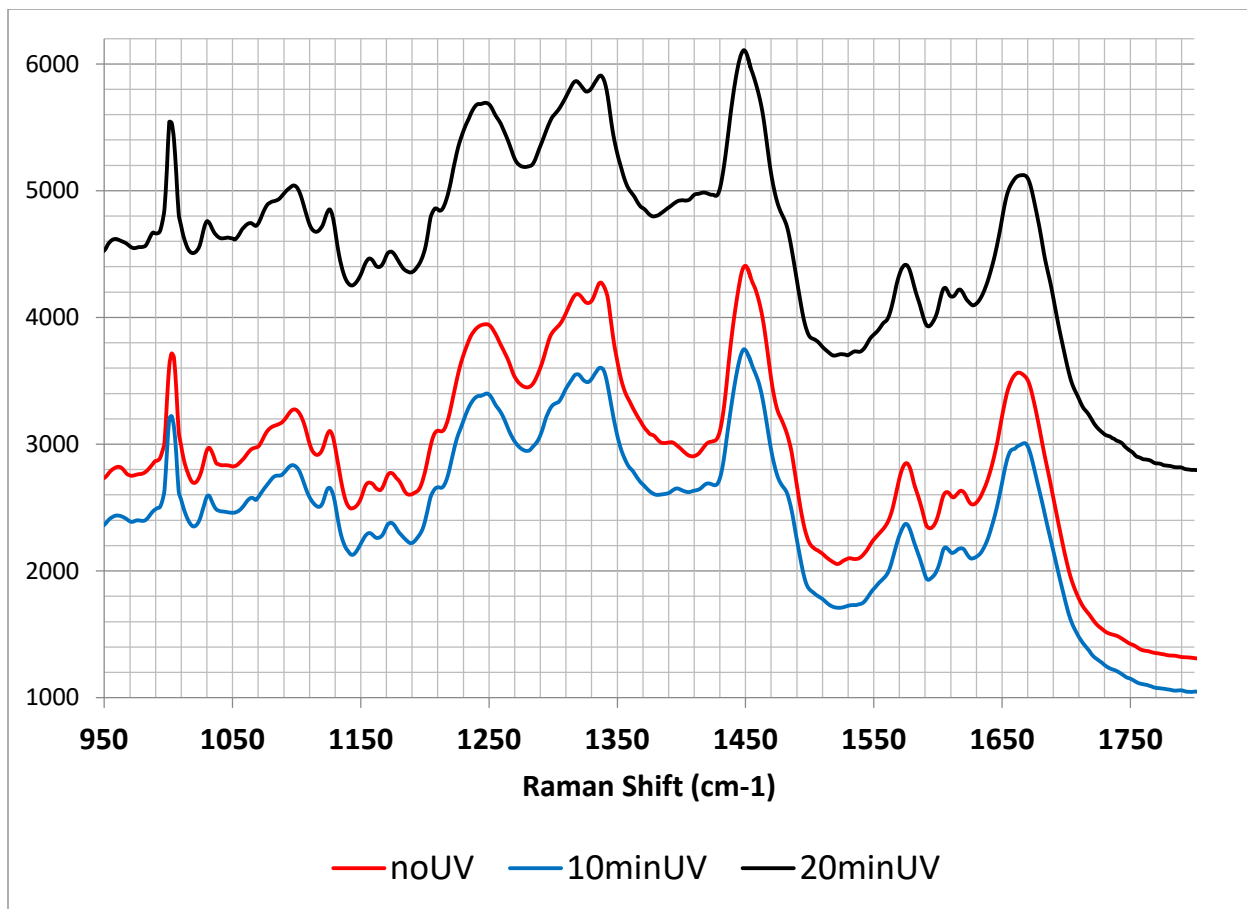
Figure 17. Raman spectra of *E.coli* in dry condition before and after UV radiation at 10 and 20 minutes
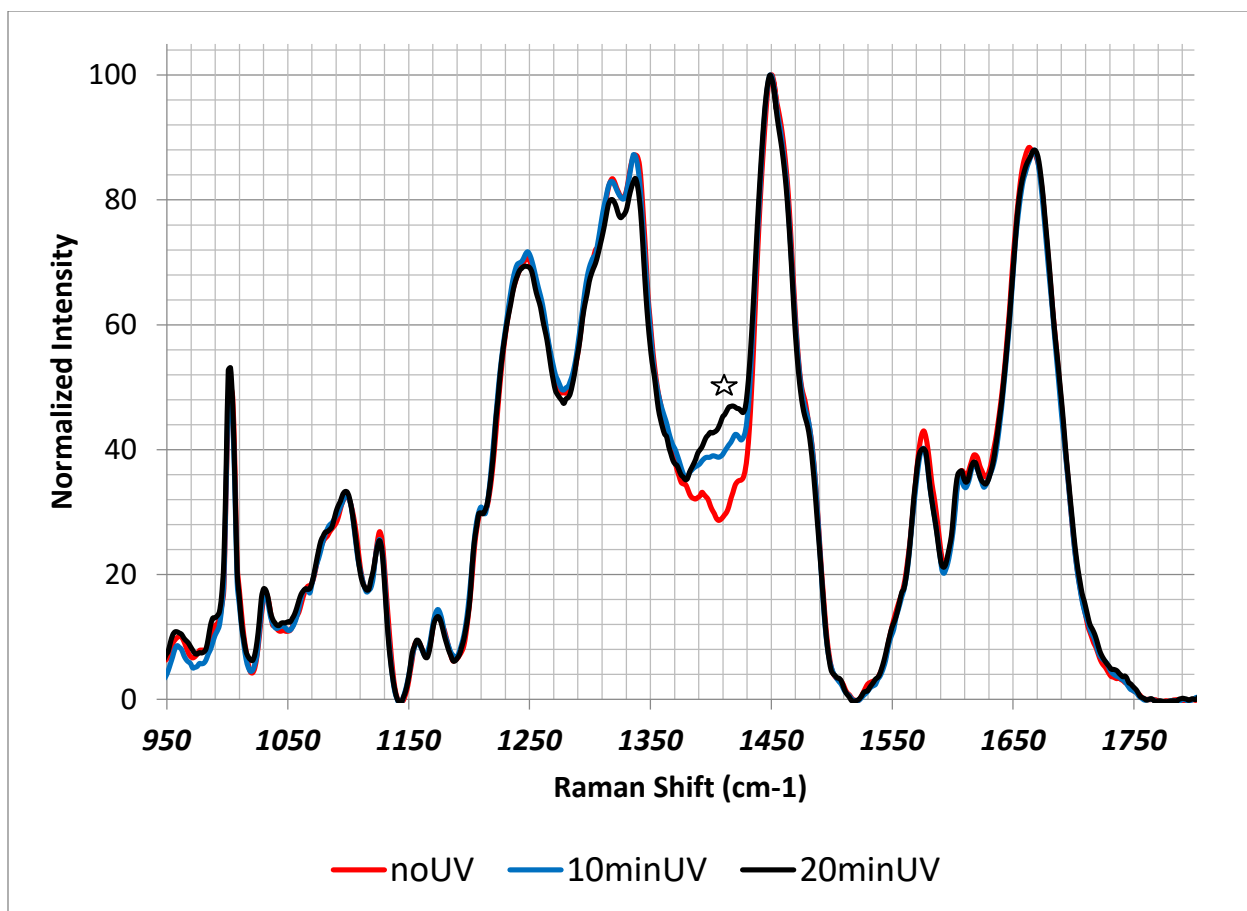
Figure 18. Raman spectra of *E.coli* in dry condition before and after UV radiation at 10 and 20 minutes after baseline removal and normalization.

The intensity of 1410 cm-1 band is plotted against the UV irradiation time used for bacterial inactivation in Figure 19. It was seen that this band increase linearly with increasing UV dose. Figure 20 showed that when intensity of 1410 cm-1 band was increased, the CFU count of bacteria solution was decreased exponentially in the same proportion. The more bacteria killed by UV radiation, the more photoproducts were detected.
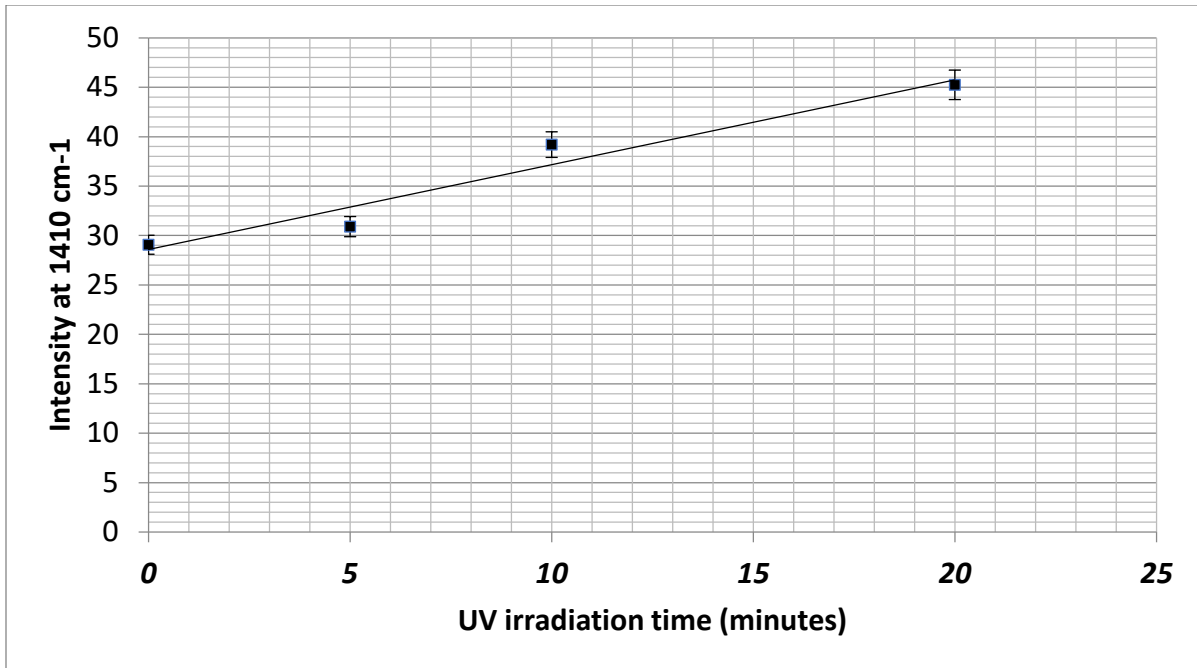
Figure 19. Change in intensity of 1410 region versus UV irradiation time

$$y = 9E+07e^{-0.611x}$$
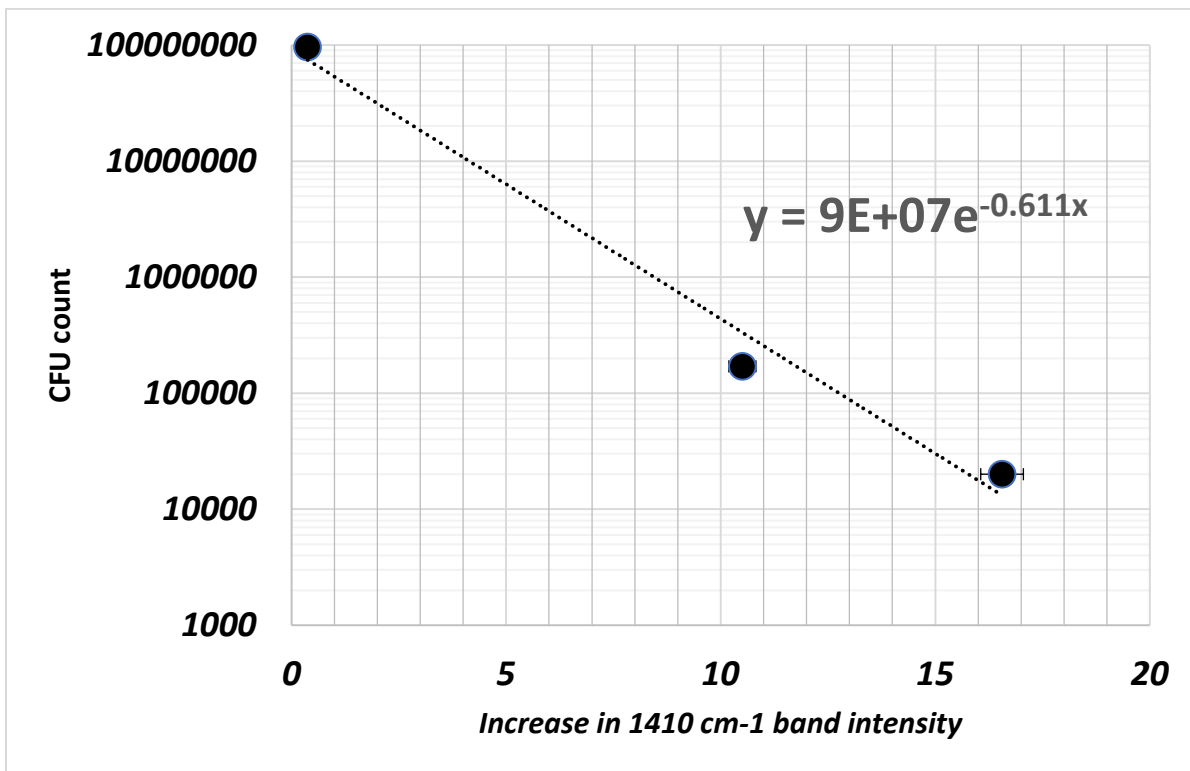
Figure 20. Change in intensity of 1410 cm-1 band versus CFU counts

These results revealed that Raman spectral features can be used to determine live and dead bacteria fraction. Increase in intensity of the 1410 cm-1 band can be used to estimate the amount of live bacteria in a given sample after UV irradiation.

Principal Component Analysis of Raman spectra data

PCA score plots and principal components obtained after analysis are presented in the Figures 21 and 22, respectively. The corresponding Colony Forming Units (CFU) of bacteria are indicated in the Figure 21.
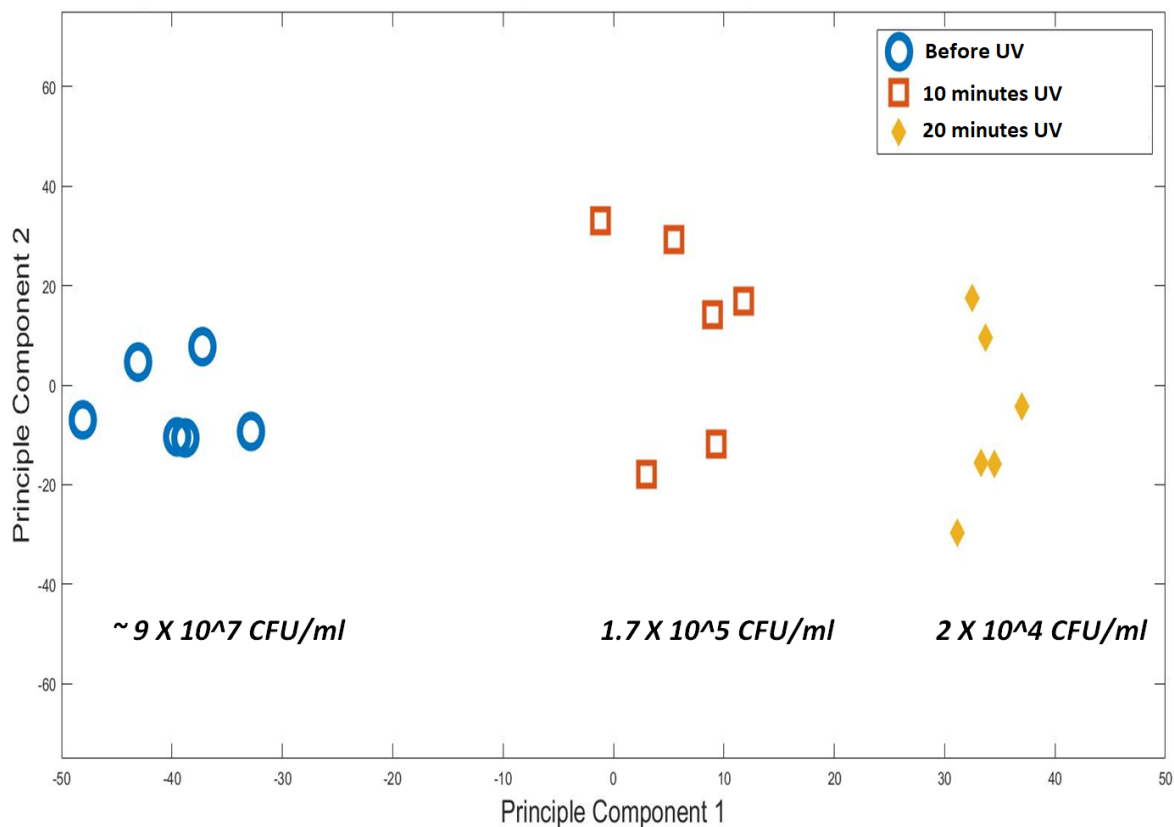
Figure 21. PCA score plots for Raman spectra of *E.coli* after UV irradiation.
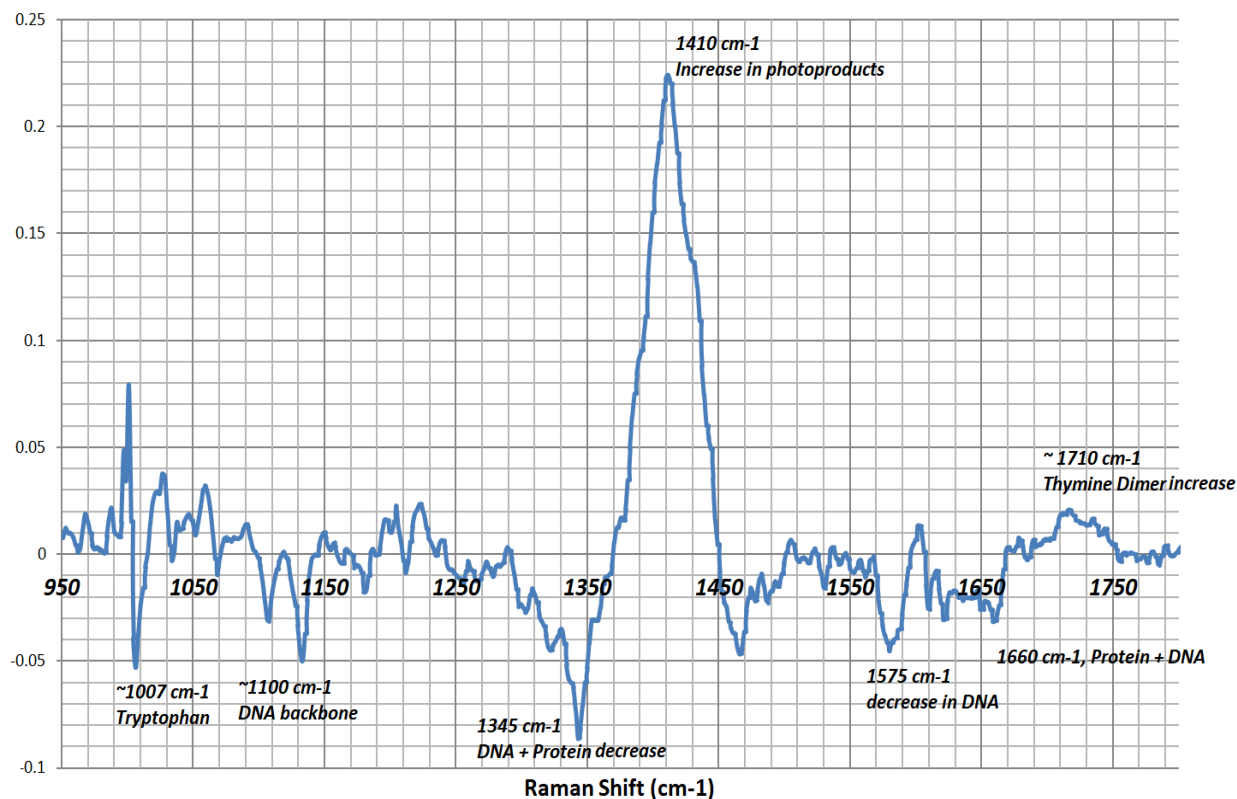
Figure 22. Principal Component 1 plot, obtained from PCA analysis

Figure 21 shows that after UV irradiation, the spectra are shifted to the right along the principal component 1 axis. From the PCA analysis of Principal component 1 (Figure 22), it is clearly seen that there are changes in several bands corresponding to DNA, proteins and a 1410 cm-1 band of the photoproducts. Adenine and Guanine at 1570 cm-1, Thymine and tryptophan around 1350 cm-1, DNA backbone around 1100 cm-1, and a rising band around 1710 cm-1 corresponding to Thymine dimers.

It has been reported that UV radiation cause thymine dimer [12]. Thymine and thymine dimer were prepared and then analyzed using Ramam spectroscopy (Figure 23). These results show that the Raman spectra of thymine show intense peaks at 1350 cm-1 and 1670 cm-1

whereas thymine dimer shows major peak at 1710 cm-1, but not at 1350 cm-1 or 1670 cm-1. These changes were observed in principal component 1, where a sharp decrease at the 1350 cm-1 of thymine band and an increase at the 1710 cm-1 of thymine dimer band were observed (see Figure 23).
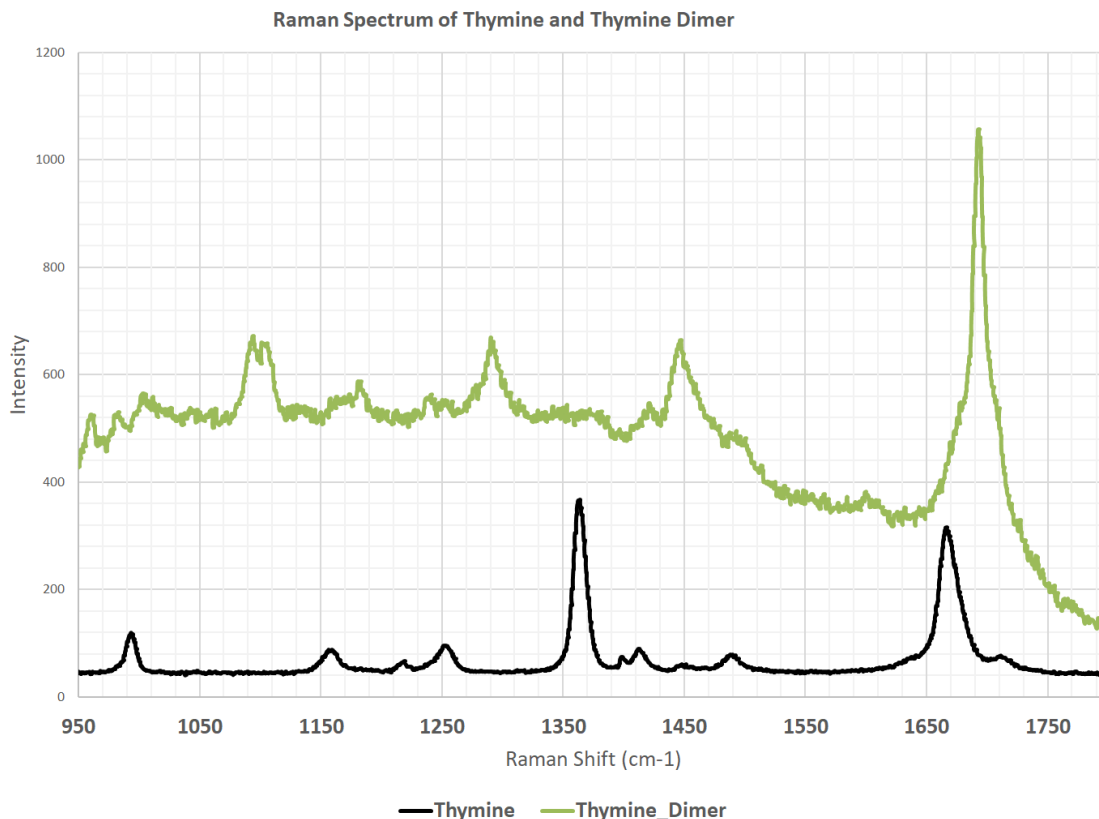
Figure 23. Raman spectrum of Thymine and Thymine dimers.

Results obtained after 280 nm UV LED irradiation

With UV LED irradiation (280 nm, 0.2 mW/cm2), changes in Raman spectra of *E.coli* similar to those obtained with mercury lamp irradiation (lines in 250-380 nm band, 2mW/cm2) for comparable UV doses were observed. Figure 24 shows the changes in the Raman spectra of *E.coli* bacteria after irradiation with 280 nm LED at different intervals of time. After UV

irradiation, a rising band around 1410 cm-1 was detected. This band increased continuously with increase in UV irradiation time.
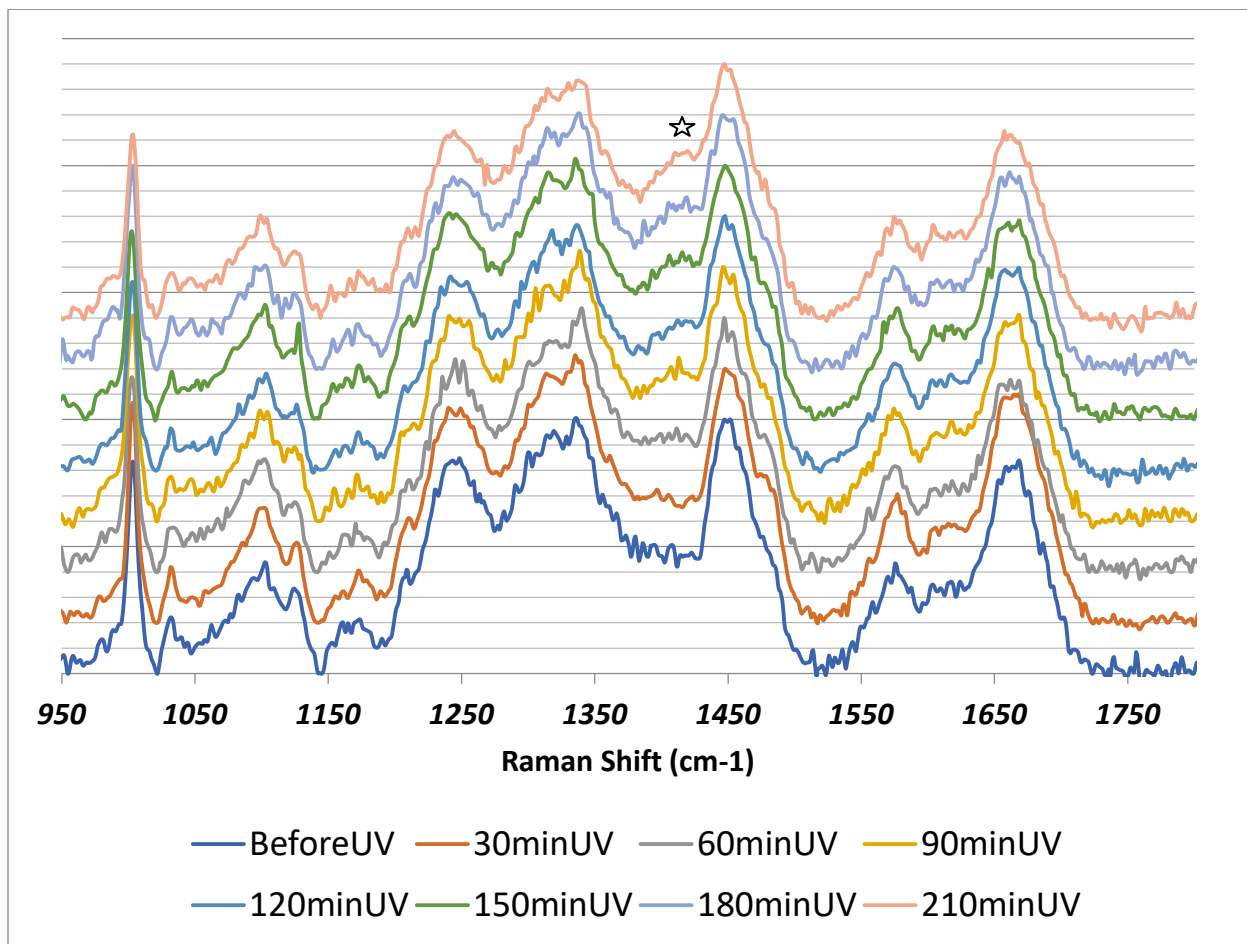
Figure 24. Changes in Raman spectra of *E.coli* bacteria after irradiation with 280 nm LED (0.2 mW/cm2). Spectra were baseline removed and normalized to lipid peak. Spectra are vertically shifted for clarity.

The intensity of 1410 cm-1 band is plotted against the UV LED irradiation time (280 nm, 0.2 mW/cm2) in Figure 25. Similar to the observation after irradiation with mercury lamp, it was observed that this 1410 cm-1 band increased linearly with irradiation time.
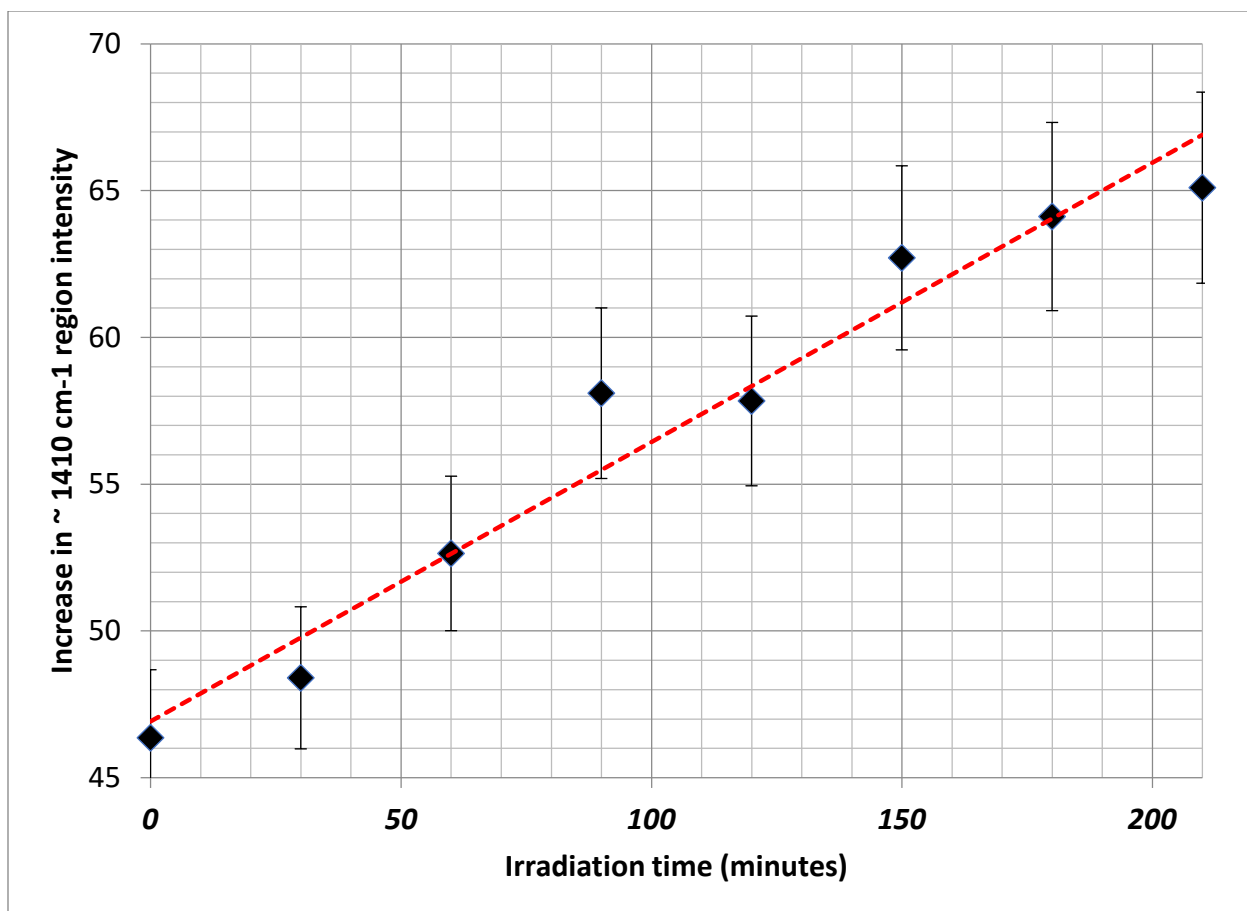
Figure 25. Trend of increase in 1410 cm-1 region intensity with time

Effects of ultraviolet radiation on proteins studied through Raman spectroscopy

In order to verify if the 1410 cm^{-1}photoproducts are proteins photoproducts, egg ovalbumin (pure protein) solution was irradiated with ultraviolet radiation and its Raman spectrum was compared to non-irradiated ovalbumin protein. A band around 1410 cm-1 was detected in pure ovalbumin protein Raman spectrum after UV irradiation (Figure 26).

Therefore, this is concluded that rise of 1410 cm^{-1} band is a major contributor from protein photoproducts. This is not surprising as 55% weight of bacteria is proteins.

It has been shown earlier [1] that bacterial fluorescence from tryptophan and tyrosine can be used to determine live and dead bacteria. When bacteria are exposed to UV light, tryptophan

40

and tyrosine undergo denaturization resulting in reduction in bacteria fluorescence and there was a quantitative relationship between cell death and decrease in bacteria fluorescence from tryptophan and tyrosine.

It is known that ultraviolet (UV) light kills cells by damaging their DNA. UV light initiates a reaction between two molecules of thymine to form the thymine dimer resulting in DNA damage which results in inability of bacteria to replicate [18]. There is less emphasis on the interaction of ultraviolet radiation with protein of the bacterial cell. Recently, when oxidative protein damage (carbonylation) induced by Ultraviolet radiation has been used as a tool to asses bacteria and other prokaryotic cells death [19],[20],[21], it was shown that protein damage caused the loss of maintenance functions of bacterial cells, including DNA repair [19]. It was also proposed that protein damage, not genomic (DNA) damage, correlates with eukaryotic and prokaryotic cell death after irradiation with UVC radiation [19].

Our experiments have shown that the effects of ultraviolet light on proteins, which constitute 55% of bacteria's weight, are significant. Protein photoproducts can be used to determine live and dead bacteria after UV radiation.
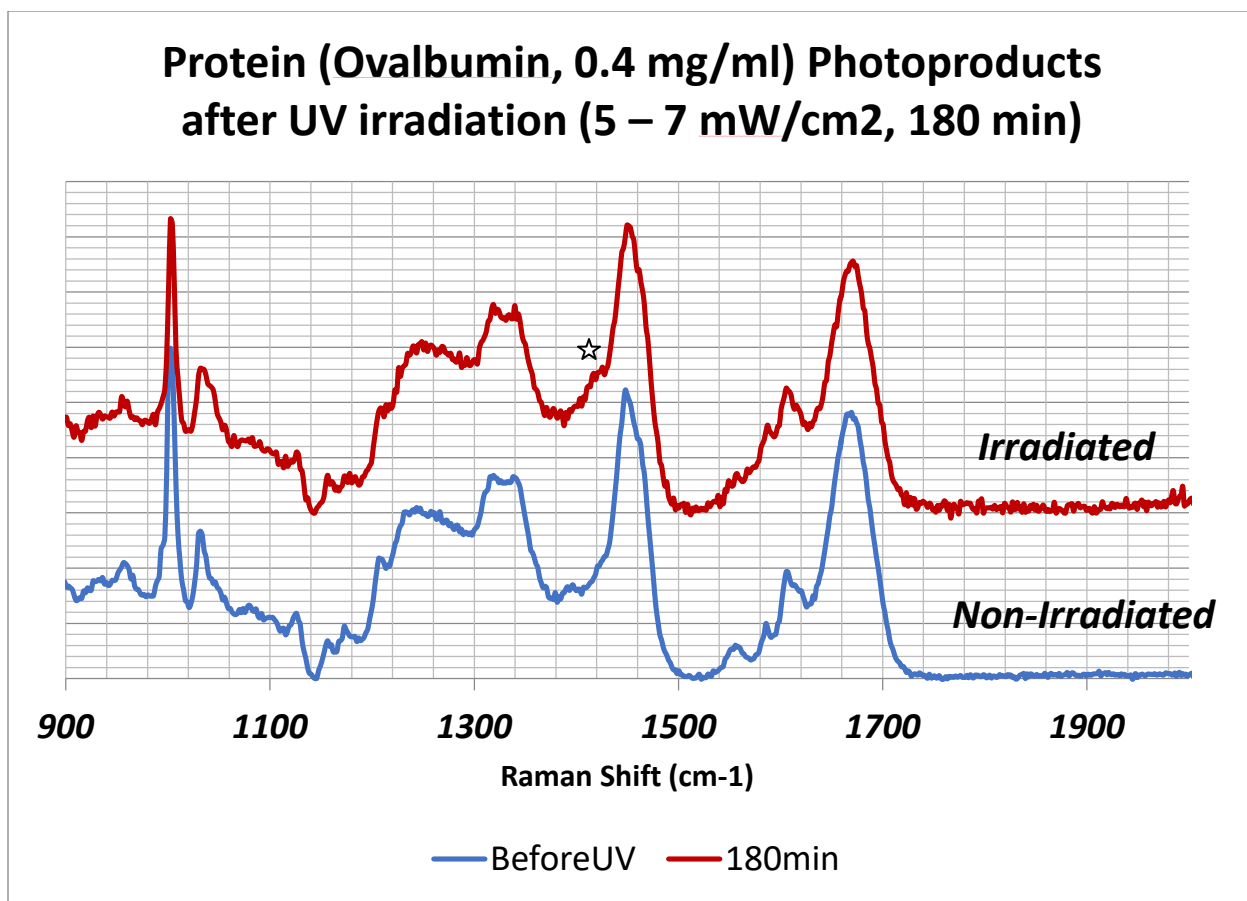
Figure 26. Changes in Raman spectra of pure protein (egg ovalbumin) with UV irradiation. Spectra are vertically shifted for clarity.

Identification of different bacteria with Raman spectroscopy

Raman spectroscopy is a powerful tool not only for determining live and dead bacteria but also for the identification of bacterial strains. Raman spectra and PCA score plot of *E.coli*, *Bacillus* and the mixture of both bacteria is shown in Figure 27. These spectra were baseline removed as per procedure described in Appendix A and were normalized to lipid peak at 1450 cm-1, then subjected to PCA analysis. Principal components obtained from PCA analysis are shown in Figure 28.
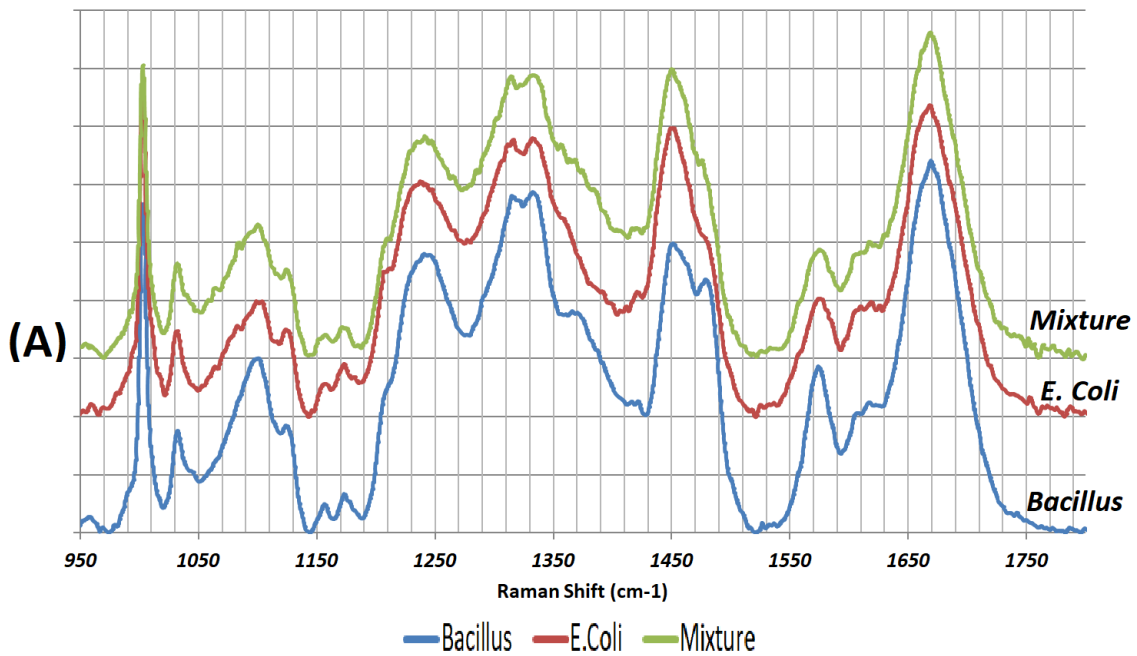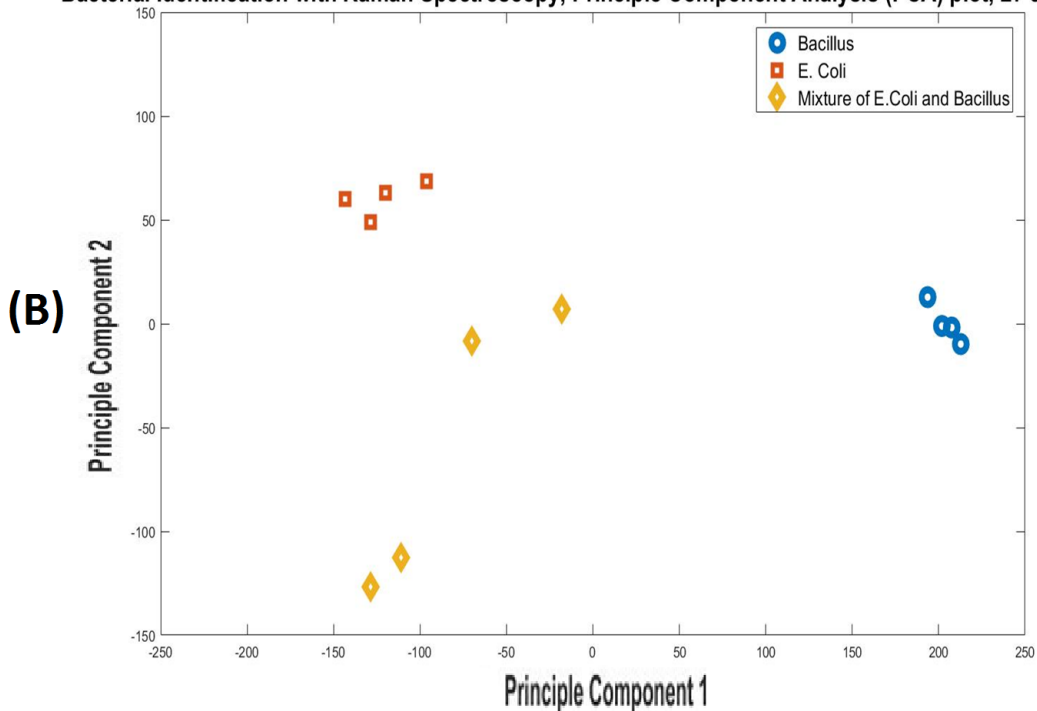
Figure 27. (A) Average Raman spectra of *E.coli* bacteria, *Bacillus* bacteria & their mixture (spectra are vertically shifted for clarity) and (B) PCA Score plot showing clustering and separation of these bacterial strains
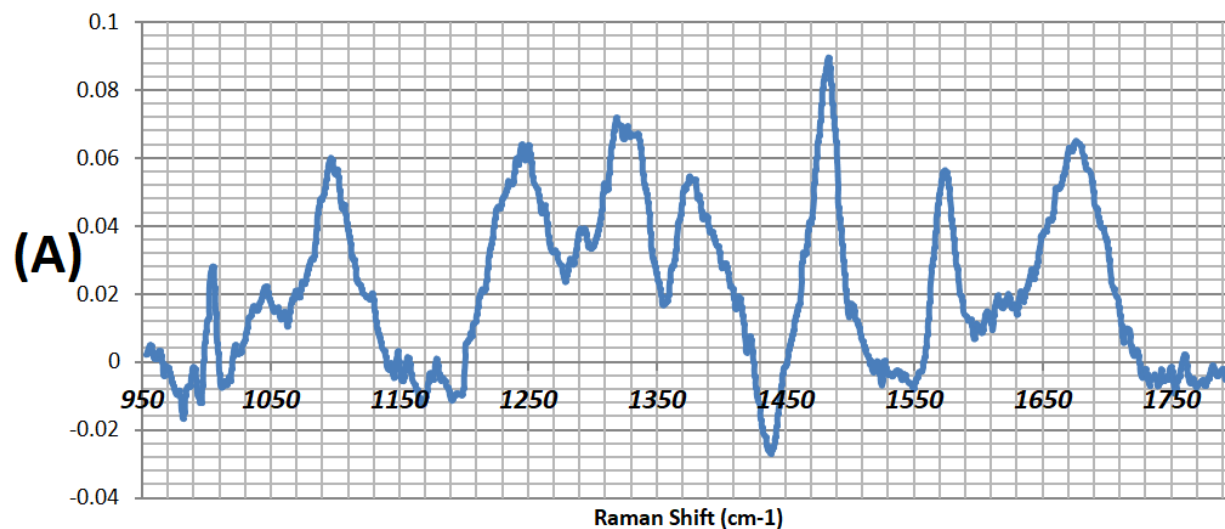
Figure 28. (A) Principal components 1 and (B) Principal component 2 obtained from PCA analysis for bacterial strain identification

Effects of ultraviolet radiation on bacteria and protein studied through fluorescence and synchronous fluorescence spectroscopy

In order to further study the effects of UV radiation on bacteria and protein, *E.coli* bacteria and ovalbumin protein were studied through fluorescence and synchronous fluorescence spectroscopy. It was observed in bacteria fluorescence, the rise of a broad band around 450 nm region with increasing UV Dose (Figure 29, inset). This increase was more clearly observed in synchronous fluorescence spectra taken with $\Delta\lambda = 65\ nm$ (Figure 30 A, inset). It is known that tryptophan photoproducts such as N-formylkynurenine and Kynurenine, tyrosine photoproduct such as dityrosine fluoresces around 450 nm [23][24] and similar increase was observed in UV irradiated ovalbumin protein (Figure 30 B, inset). Therefore, it can be estimated that this broad 450 nm band has a major contribution from tryptophan, tyrosine and other protein photoproducts.
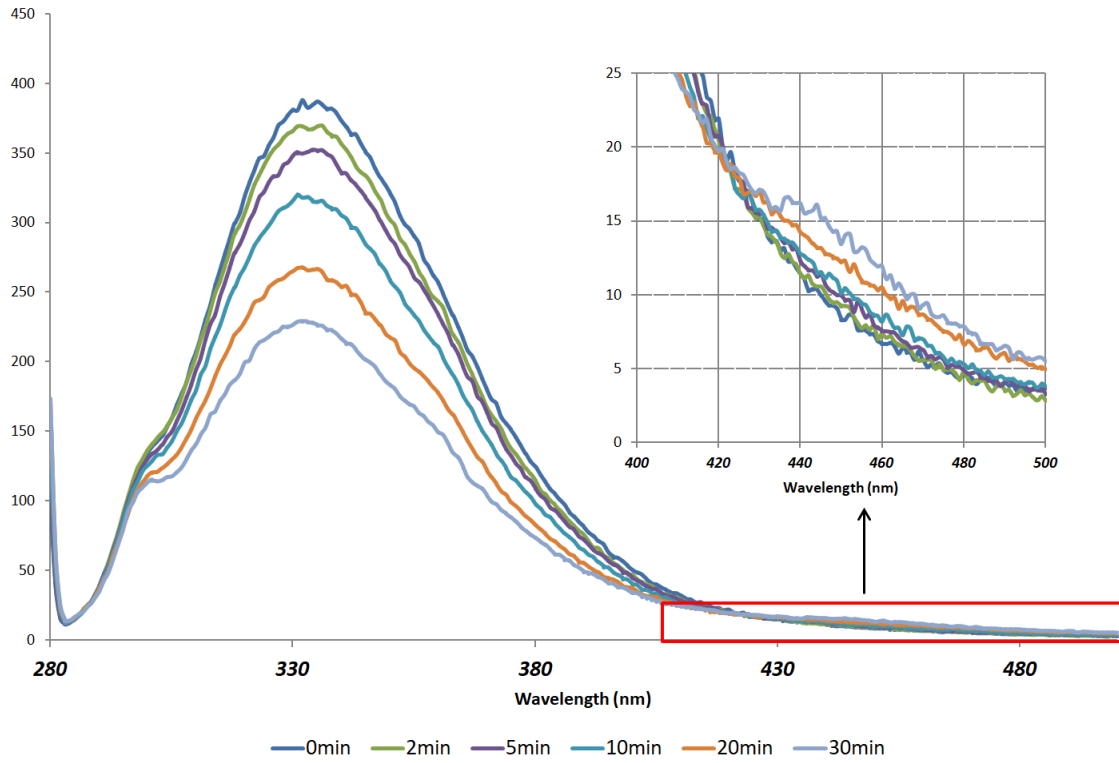
Figure 29. Change in E.coli fluorescence (excitation at 270 nm) with UV Irradiation (6mW/cm2) for different times
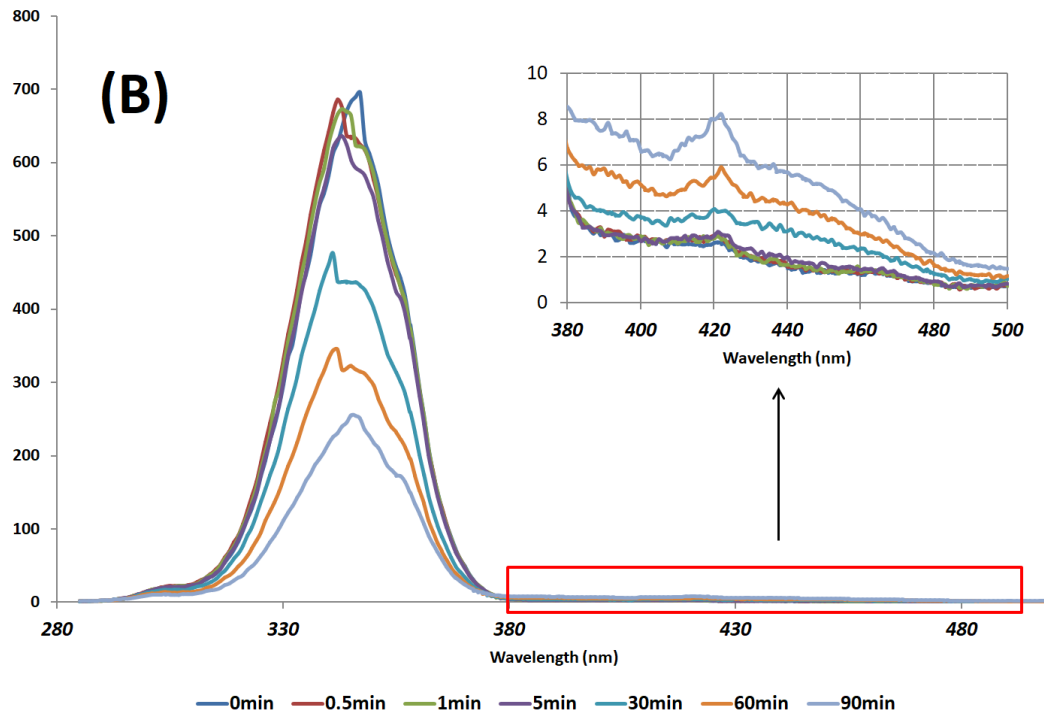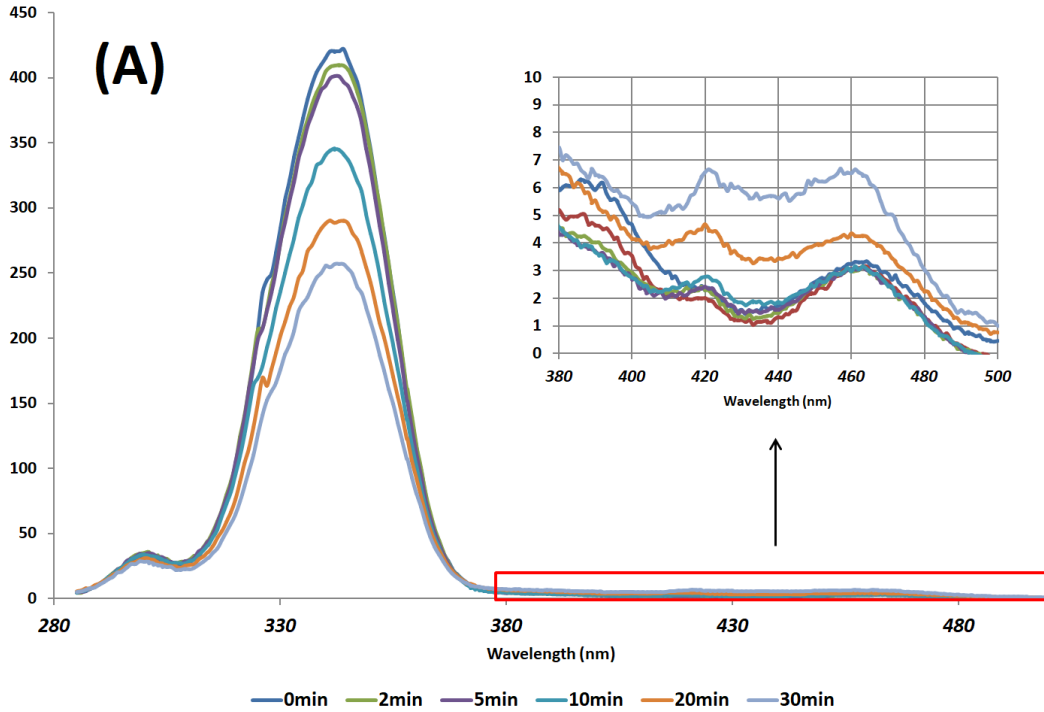
Figure 30. Increase in fluorescence band in the blue region with UV irradiation (6 mW/cm2) for (A) *E.coli* **Bacteria (OD600 ~ 0.1), inset and (B) Ovalbumin protein (0.4 mg/ml), inset. Spectra shown are synchronous fluorescence spectra with Δλ = 65 nm**

These protein photoproducts, such as N-formylkynurenine and Kynurenine are shown to be absorbing the light of wavelengths around 350 nm [26]. Since, protein photoproducts absorb around 350 nm (and fluoresce around the 450 nm region) and proteins absorb at 280 nm (and fluoresce around the 340 nm), this characteristic of protein and their photoproducts can be used to determine quantitatively protein damage in a bacteria which can then be correlated with the live and dead bacteria in a sample after treatment with UVC radiation. As proteins degrade with UVC radiation, their fluorescence at 340 nm decreases whereas the protein photoproducts fluorescence at 450 nm will increase. Fluorescence excited at 270 nm and 350 nm of *E.coli* bacteria were recorded and plotted as a function of irradiation time (Figure 31 A and 31 B). Figure 31 C shows how the ratio of protein fluorescence to protein photoproducts fluorescence decreases with UV irradiation time. The ratio was found to be decreasing exponentially with UV irradiation.
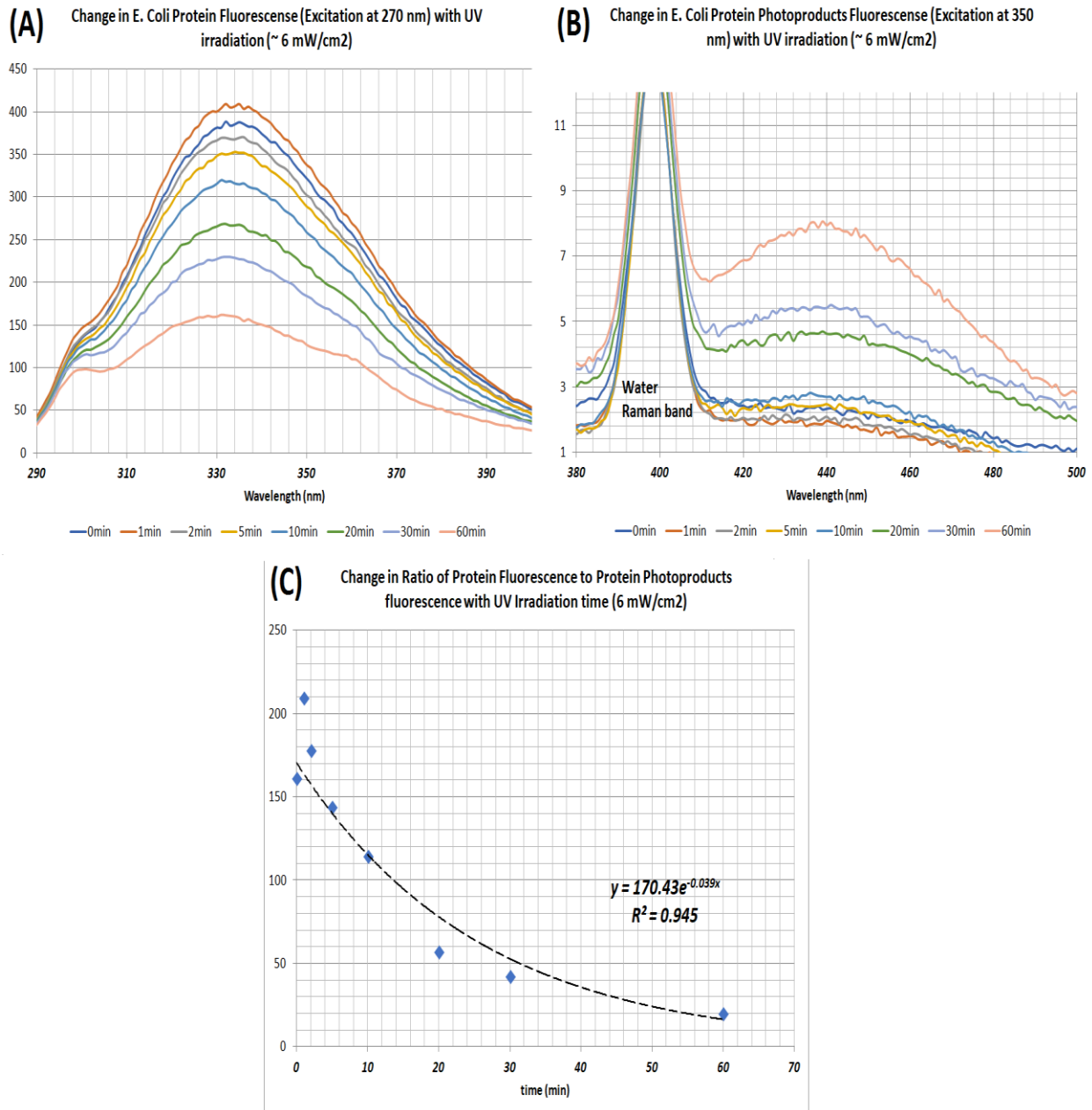
Figure 31. (A) Intensity of *E.coli* fluorescence band (excited at 270 nm) as a function of UV irradiation time. (B) Intensity of *E.coli* photoproduct fluorescence band (excited at 350 nm) as a function of UV irradiation time. (C) Ratio of intensities of *E.coli* fluorescence band and *E.coli* photoproduct.

CHAPTER VI

CONCLUSION

In this work a novel handheld device was successfully designed and constructed which can be used to determine live and dead bacteria in-situ, within minutes. Additionally, it was shown that Raman spectroscopy can be used to determine live and dead bacteria after inactivation with ultraviolet light from a mercury lamp or from a 280 nm UV LED. Change in DNA and formation of protein photoproducts after UV inactivation of bacteria was verified with Raman spectroscopy. Raman spectroscopy was also used to identify different bacteria strains. tryptophan and tyrosine photoproducts were detected after UV inactivation of bacteria using fluorescence and synchronous fluorescence spectroscopy. It was also shown that ratio of tryptophan & tyrosine to their photoproducts can be calculated using two LED excitation method at 270 nm and 350 nm and this ratio decreases continuously with UV irradiation of the bacteria samples which can also be utilized to calculate live and dead bacteria in a sample.

REFERENCES

[1] Runze Li, Umang Goswami, Maria King, Jie Chen, Thomas C. Cesario, and Peter M. Rentzepis, In situ detection of live-to-dead bacteria ratio after inactivation by means of synchronous fluorescence and PCA, PNAS, January 23, 2018, vol. 115, no.4, 668–673.

[2] Sohn M, Himmelsbach DS, Barton FE, 2nd, and Fedorka-Cray PJ, Fluorescence spectroscopy for rapid detection and classification of bacterial pathogens. Appled Spectroscopy, 2009, vol. 63, no. 11, 1251–1255

[3] Ammor S, Yaakoubi K, Chevallier I, and Dufour E, Identification by fluorescence spectroscopy of lactic acid bacteria isolated from a small-scale facility producing traditional dry sausages, Journal of Microbiological Methods, November 2004, vol. 59, no. 2, 271-281

[4] Bhatta, H. and Goldys, E. M. and Learmonth, Robert P, Use of fluorescence spectroscopy to differentiate yeast and bacterial cells. Applied Microbiology and Biotechnology, 2006, vol. 71, Issue 1, 121-126

[5] McNamara L, Health care-associated infection, American Journal of Critical Care, January 2009, vol. 18, no. 1, 41

[6] Herve Abdi and Lynne J. Williams, Principal component analysis, July/August 2010, WIREs Computational Statistics, Volume 2, 433-459

[7] Ethem Alpaydın, Introduction to Machine Learning, 2010, MIT press, Second Edition, 113-120

[8] Melanie J. Harris, Nalin Chandra Wickramasinghe, David Lloyd, J. V. Narlikar, P. Rajaratnam, et al., Detection of living cells in stratospheric samples, Proc. SPIE 4495, Instruments, Methods, and Missions for Astrobiology IV, 5 February 2002, 191-198

[9] O.U. Mason, Tatsunori Nakagawa, Martin Rosner et al, First Investigation of the Microbiology of the Deepest Layer of Ocean Crust, PLoS One, November 2010, vol. 5, Issue 11, 1-11

[10] David J. Smith, Jayamary Divya Ravichandar, Sunit Jain et al., Airborne Bacteria in Earth's Lower Stratosphere Resemble Taxa Detected in the Troposphere: Results From a New NASA Aircraft Bioaerosol Collector (ABC), Frontiers in Microbiology, August 2018, Volume 9, Article 1752, 1-20

[11] F. C. Neidhardt(ed.), et al., *Escherichia coli* and *Salmonella*: cellular and molecular biology, ASM Press, Washington, D.C, Vol. 1, 2nd edition, 14

[12] Rajesh P. Rastogi, Richa, Ashok Kumar, Madhu B. Tyagi, and Rajeshwar P. Sinha, Molecular Mechanisms of Ultraviolet Radiation-Induced DNA Damage and Repair, Journal of Nucleic Acids, December 2010, vol. 2010, Article ID 592980, 1-32

[13] J.H. Clark, The denaturation of egg albumin By Ultra- violet radiation, The Journal of General Physiology, 1935, vol. 19 (2), 199-210

[14] Lars Redecke, Stephan Binder, Mohammed I.Y. Elmallah et al, UV-light-induced conversion and aggregation of prion proteins, Free Radical Biology & Medicine, 2009, vol. 46, 1353–1361

[15] Manuel Correia., Viruthachalam Thiagarajan, Isabel Coutinho et al, Modulating the Structure of EGFR with UV Light: New Possibilities in Cancer Therapy, PLoS One, November 2014, vol. 9, Issue 11, 1-15.

[16] Michael J. Daly, Elena K. Gaidamakova , Vera Y. Matrosova et al, Protein oxidation implicated as the primary determinant of bacterial radioresistance, PLoS Biology, April 2007, vol. 5, Issue 4, 0769-0779

[17] Kendrick C. Smith, Photochemical Reactions of Thymine, Uracil, Uridine, Cytosine And Bromouracil In Frozen Solutlon And In Dried Films, Photochemistry and Photohiology, 1963, vol. 2, 503-517

[18] R. B. Setlow, P. A. Swenson and W. L. Carrier, Thymine Dimers and Inhibition of DNA Synthesis by Ultraviolet Irradiation of Cells, Science, 13 Dec 1963, Vol. 142, Issue 3598, 1464-1466

[19] Andrea Nikolić , Matea Perić, Romain Ladouce et al, Death by UVC Light Correlates with Protein Damage in Isogenic Human Tumor Cells: Primary Tumor SW480 versus its Metastasis SW620, Journal of Proteomics & Computational Biology, March 2016, vol. 2, Issue 1, 01-012

[20] Anita Krisko and Miroslav Radman, Protein damage and death by radiation in *Escherichia coli* and *Deinococcus radiodurans*, PNAS, August 10, 2010 , vol. 107, no. 32, pp 14373–14377

[21] Michael J. Daly, Death by Protein damage in irradiated cells, DNA Repair, 2012, vol. 11, 12-21

[22] Isabella Dalle-Donnea, Ranieri Rossi , Daniela Giustarini et al, Protein carbonyl groups as biomarkers of oxidative stress, Clinica Chimica Acta, 2003, vol. 329, 23–38

[23] Linda V. Sinclair, Damien Neyens, George Ramsay et al, Single cell analysis of kynurenine and System L amino acid transport in T cells, Nature Communications, 2018, vol. 9, 1981-1991

[24] Antoinette Pirie, Fluorescence of N'-Formylkynurenine and of Proteins Exposed to Sunlight, Biochem. J. , 1972, vol. 128, 1365-1367

[25] Chamani Niyangoda , Tatiana Miti , Leonid Breydo et al, Carbonyl-based blue autofluorescence of proteins and amino acids, PLoS One, May 2017, 1-15

[26] Yasutsugu Fukunaga, Yasuhiro Katsuragi, Takashi Izumi, and Fumio Sakiyama, Fluorescence characteristics of kynurenine and N'-formylkynurenine. Their use as reporters of

the environment of tryptophan 62 in hen egg-white lysozyme, The Journal of Biochemistry, July 1982, vol. 92, Issue 1, 129-141

[27] Eleana Kristo, Artan Hazizaj, and Milena Corredig, Structural Changes Imposed on Whey Proteins by UV Irradiation in a Continuous UV Light Reactor, Journal of Agricultural and Food Chemistry, 2012, vol. 60, 6204−6209

[28] Jaya Bhattacharyya and Kali P. Das, Molecular Chaperone-like Properties of an Unfolded Protein, α_s-Casein, The Journal Of Biological Chemistry, 28 May 1999, vol. 274, no. 22, 15505–15509

[29] Cicile Roselli, Alain Boussac, and Tony A. Mattioli, Direct vibrational structure of protein metal-binding sites from near-infrared Yb3+ vibronic side band spectroscopy, Proceedings of National Academy of Science USA, December 1994, Vol. 91, 12897-12901

[30] P. Rösch, M. Harz, K.D. Peschke et al, Identification of Single Eukaryotic Cells with Micro-Raman Spectroscopy, Biopolymer, 2006, vol. 82, 312-316

[31] A. Rygula, K. Majzner, K. M. Marzec et al., Raman spectroscopy of proteins: a review, Journal of Raman Spectroscopy, 13 July 2013, vol. 44, 1061-1076

[32] Hossein Heidari Torkabadi, Christopher R. Bethel, Krisztina M. Papp-Wallace et al, Following Drug Uptake and Reactions inside Escherichia coli Cells by Raman Microspectroscopy, Biochemistry, 2014, vol. 43, 4114-4121

[33] K. Christian Schuster, Ingo Reese, Eva Urlaub et al, Multidimensional Information on the Chemical Composition of Single Bacterial Cells by Confocal Raman Microspectroscopy, Analytical Chemistry, 2000, vol. 72, no. 22, 5529-5534

[34] Wei E. Huang, Robert I. Griffiths, Ian P. Thompson et al, Raman Microscopic Analysis of Single Microbial Cells, Analytical Chemistry, 2004, vol. 76, no. 15, 4452-4458

[35] Okturb et al, Raman Spectroscopy for DNA Quantification in Cell Nucleus, Cytometry Part

A , 2015, vol. 87A, pp 68-73

Baseline removal procedure

Baseline was removed using LabSpec6 software provided with HORIBA Xplora Raman system. 20 point linear fit was used to fit baseline. Points 1, 2, 3 and 4 are always on the baseline touching the spectra. Points 1, 2, 3 and 4 were connected using straight line to form the baseline. Spectrum beyond point 4 was taken as baseline.
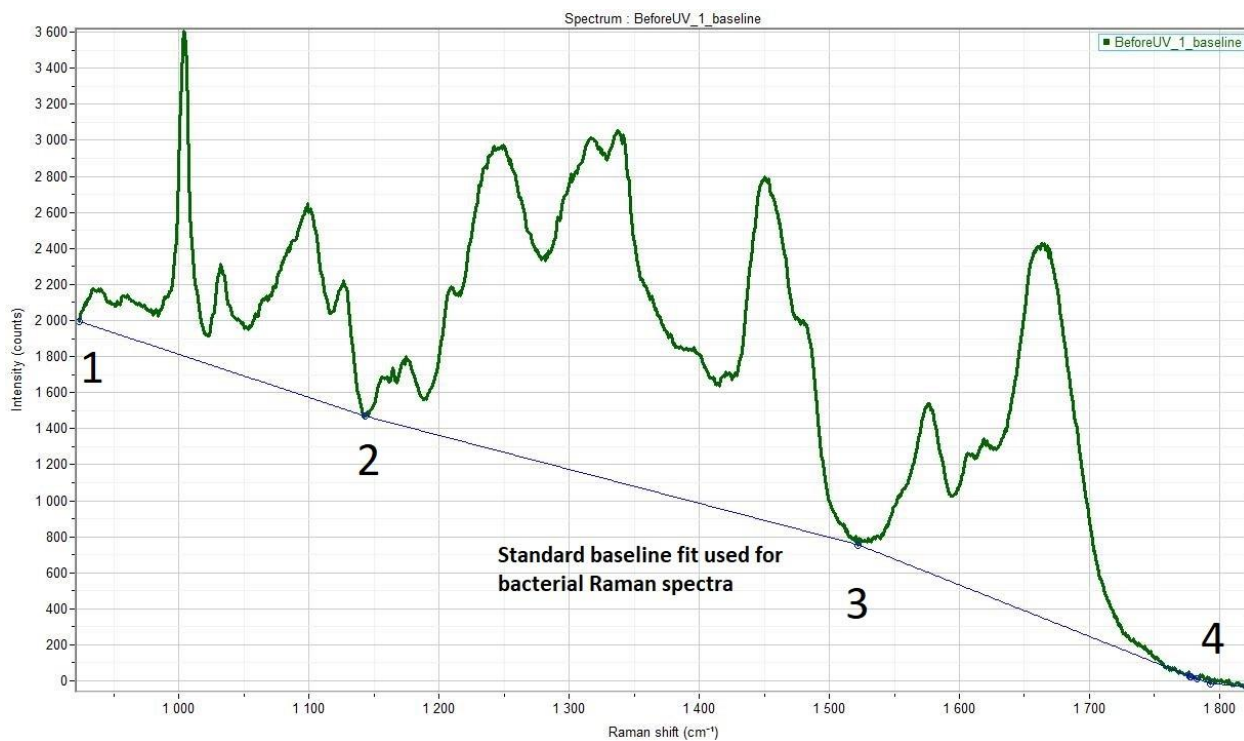

Figure 32. Standard baseline fit used for bacterial Raman spectra

APPENDIX B

Table 2. Raman Band Assignments

Raman Band (cm-1)	Assignment	Reference
1746	C=O of esters	[30]
1665	protein	[30]
	Amide I vibrations of polypeptide backbone	[31]
	C=O stretch	[32]
1608	Tyrosine (1612)	[32]
	Tryptophan (1604)	[32]
1581/1576	DNA	[30]
	G, A	[32]
	C=C, deformation of N-H, Stretching of C-N bond	[33]
	Nucleic Acid	[34]
1451	CH2 modes	[32]
	CH2, CH3 deformation vibrations	[30]
	Lipids	[34]
1334/1307	Amide III	[33]
	Tryptophan, Cα-H deformations	[31]
1232-1243	Proteins	[34]
	Amide III	[32]
1030	Phenylalanine	[31]
1172,1156,1123,1096,1030	Lipids, DNA & RNA Backbone	[32]
	Carbohydrates	[34]
1096	Phosphate mode in DNA	[35]
	-C-C-, C-O, deformation of C-O-H	[33]

Table 2 continued….

Raman Band (cm-1)	Assignment	Reference
999.66	Protein	[35]
	Phenylalanine	[34]
	Phenylalanine in proteins	[30]
850	Tyrosine in proteins	[32],[31], [35]
830	Tyrosine in proteins	[32],[31], [35]
815	Nucleic Acid in RNA C-O-P-OC in RNA backbone	[35]
780	DNA	[35]
	C,T, DNA backbone	[32]
747	Tryptophan ring vibrations	[30]
721	Adenine	[32]
667	Guanine	[32]
642	Tyrosine	[32]